A multi-scale, multi-physics approach to microquasars

Rolf Walder, Mickaël Melzani, Christophe Winisdoerffer, Doris Folini, & Jean Favre
Centre de Recherche Astrophysique de Lyon, CRAL, ENS-Lyon, France

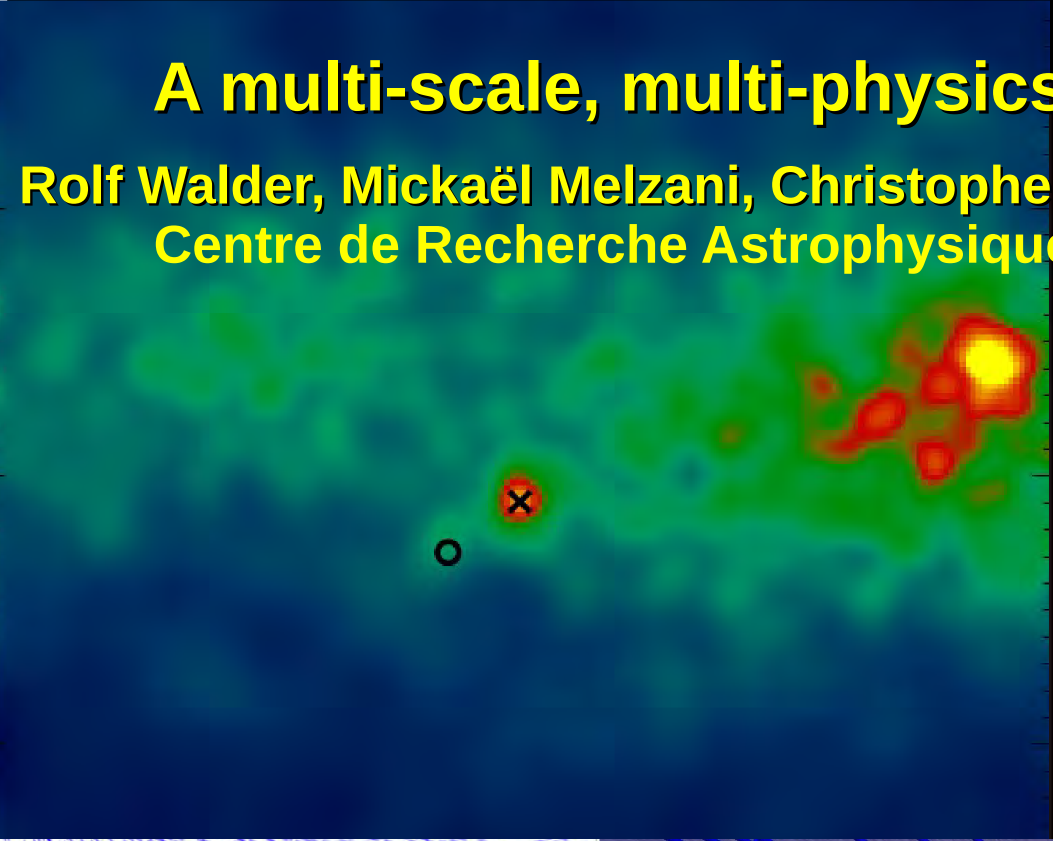

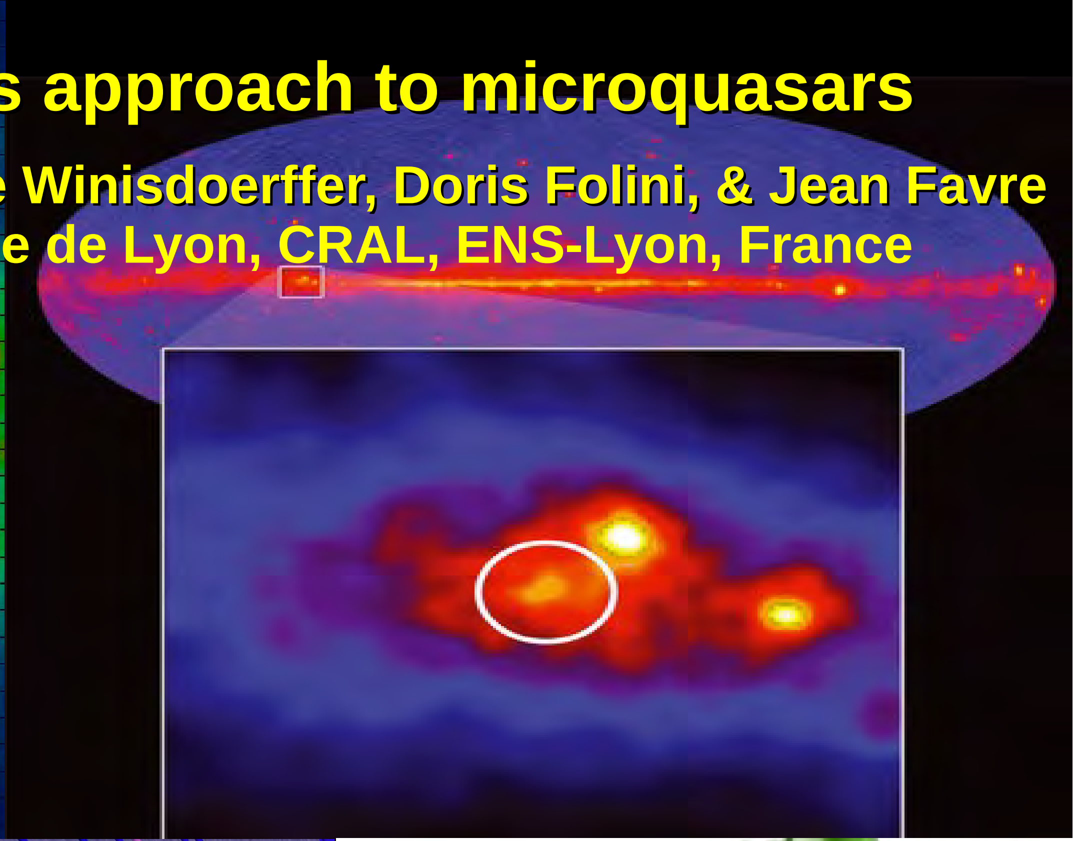

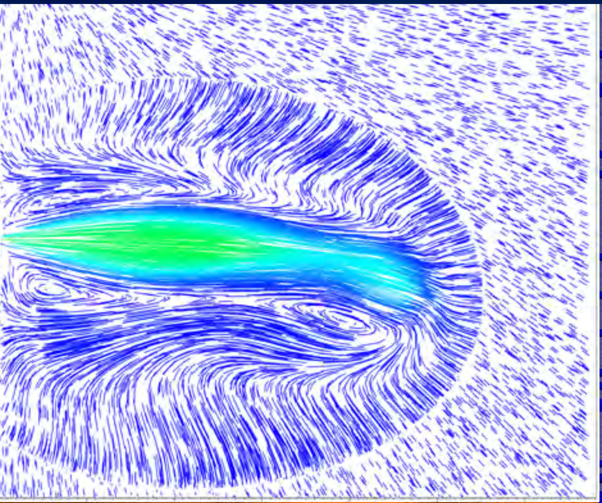

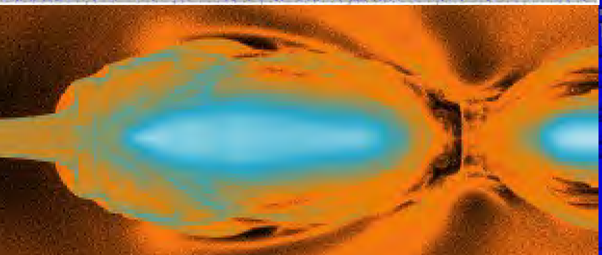

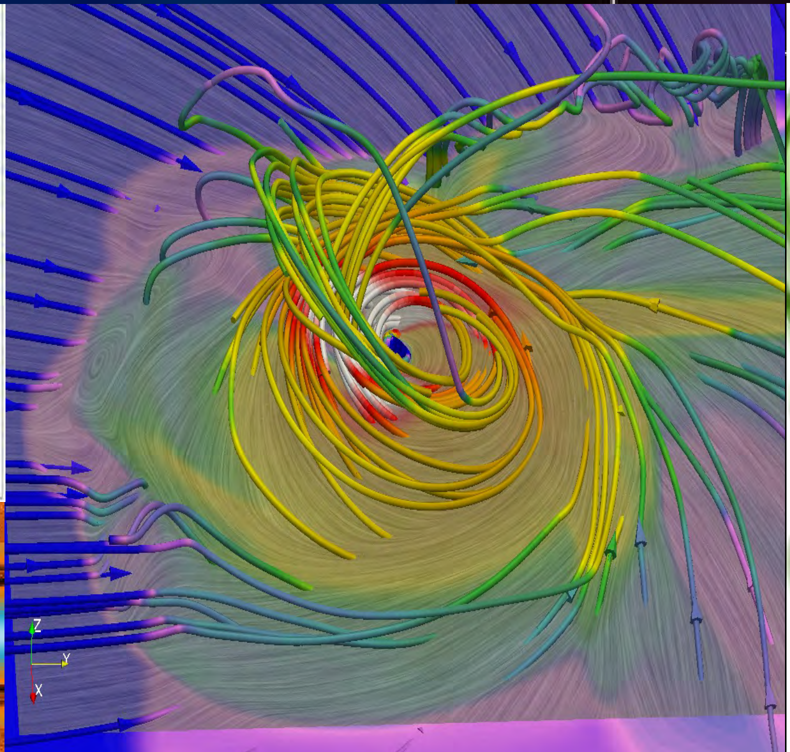

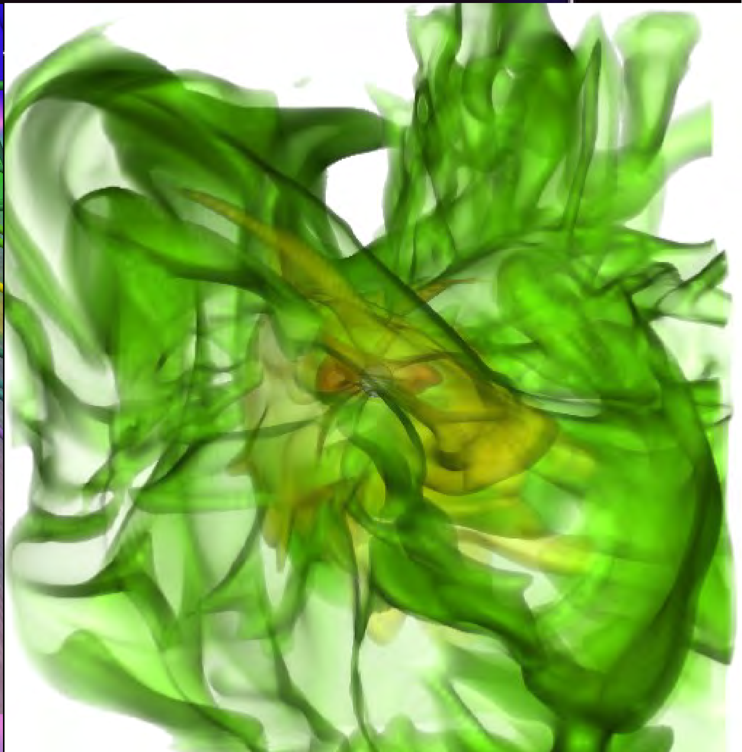

Outline

What are microquasars?

Full scale hydro-dyanmical simulations of wind-accreting Cyg X-1 : from circumbinary scale to the BH scale

Outlook: how to include more physics?

Acknowledgement:

- **Paul Grassein and Laura Mannering**
- **M. Berger, A. de Boeuf, R. Cohet, E. de Sturler, M. Gerber, S. Grossenbacher, N. Haddad, L. Huber, A. Johnson, R. LeVeque, D. Megert, P. Messmer, S. Motamen, M. Psarros, K.-M. Shuye M. Viallet**
- GENCI, Grand Equipment National de Calcul Intensiv, grant x2013046960, 1.5M hours
- PSMN, Pôle Simulation et Modélisation Numérique (méso-centre de calcul, Lyon)
- PNPS, Pôle National de la Physique Stellaire
- CSA, Commission Spécialisée Astronomie

Micro-quasars: binary systems with jets

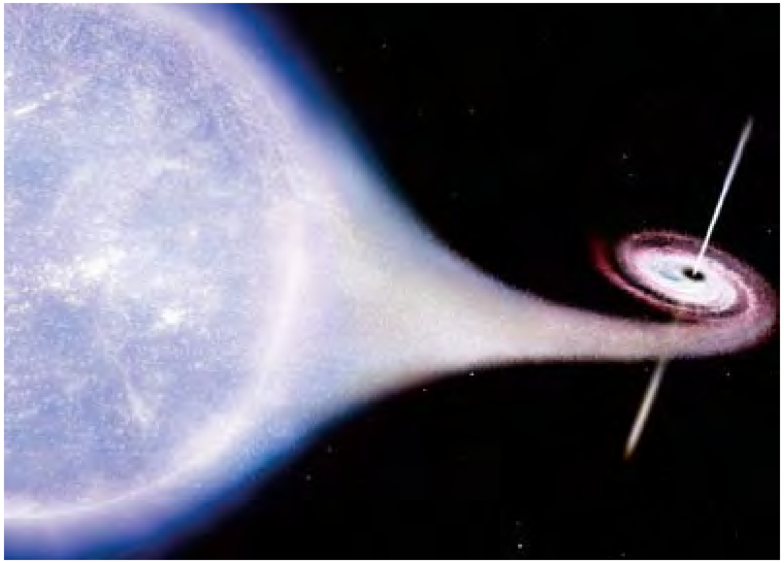

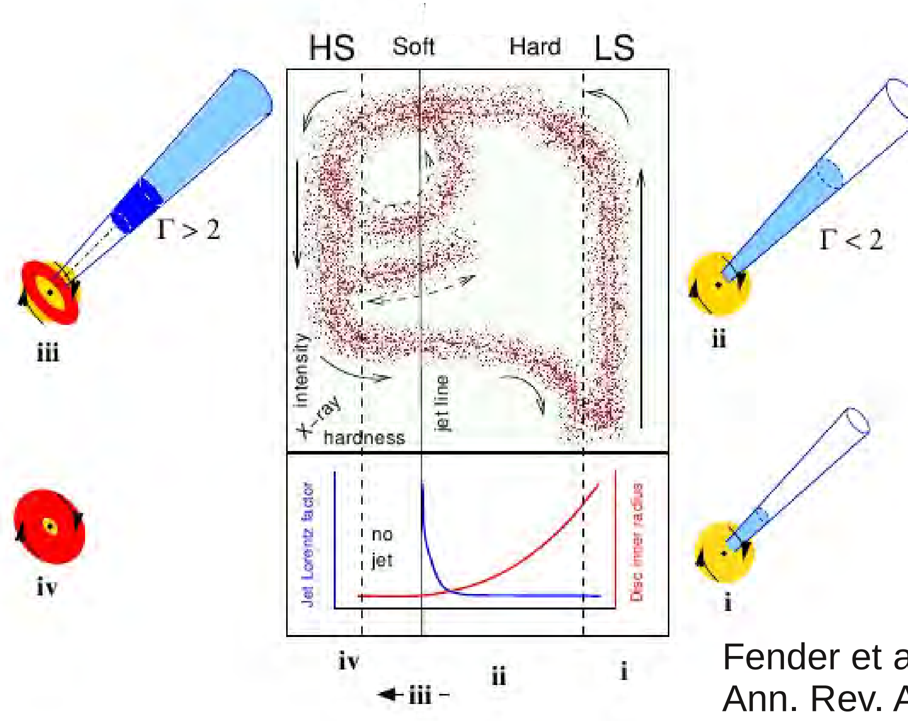

HS: High state
LS: Low state

Fender et al.
Ann. Rev. AA. 42, 317 (2004)

Many systems stay most of the time in a quiet, jet-less state.
(presumably similarly to galaxies, where AGN states are episodic.

Spectral state changes are normally not predictable.
Many suggestions for the change-trigger:
- thermal instability of the disk
- Keplerian disk (Shakura-Sunyaev disk) vs. ADAF (advection dominated acc. Flow)

Micro-quasars: binary systems with jets

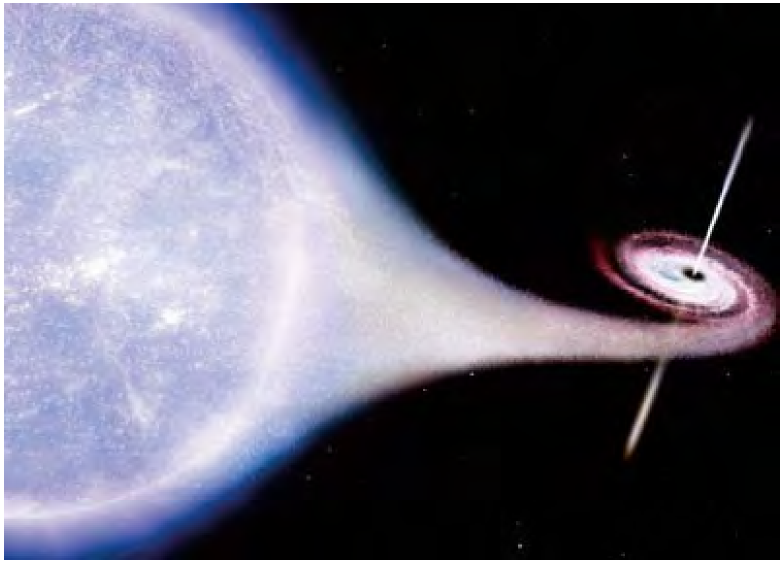

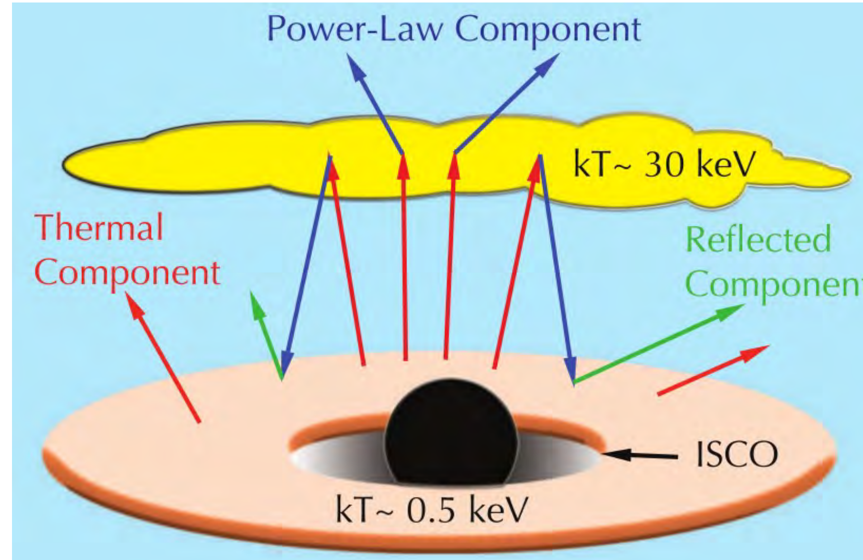

Roche potential in co-rotating frame

$$\Phi(\vec{r}) = -\frac{GM_1}{|\vec{r}-\vec{r_1}|} - \frac{GM_2}{|\vec{r}-\vec{r_2}|} - \frac{1}{2}\left(\vec{\Omega}_B \wedge \vec{v}\right)$$

Lagrange-point L_1:
lowest potential between stars

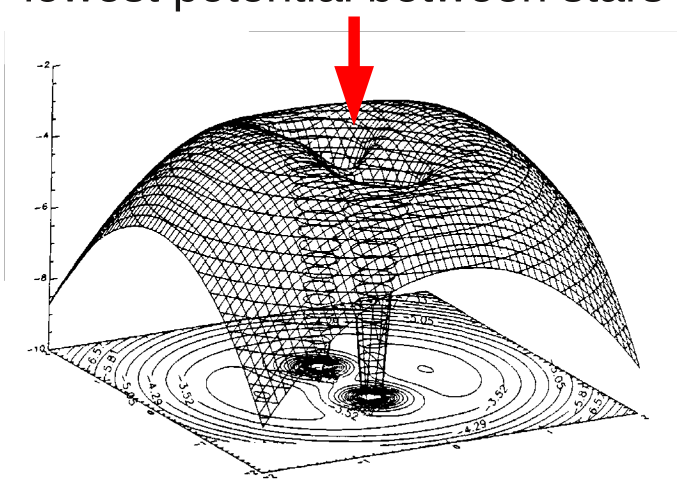

Paradigm:
smooth flow through L1 forms a
classical (Shakura&Sunyaev, 1976) disk
- geometrically thin
- optically thick
- nearly circular Keplerian orbits
- turbulent friction advects
  mass inwards and angular momentum outwards

Yet another mode of mass transfer: winds

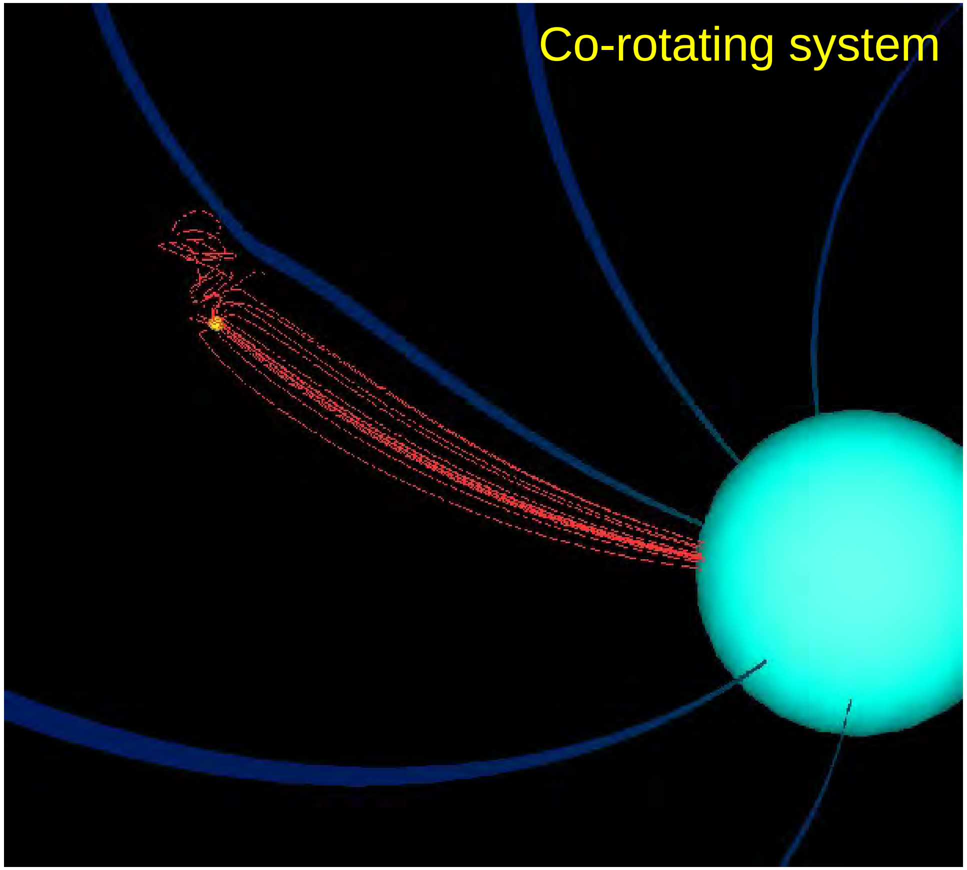

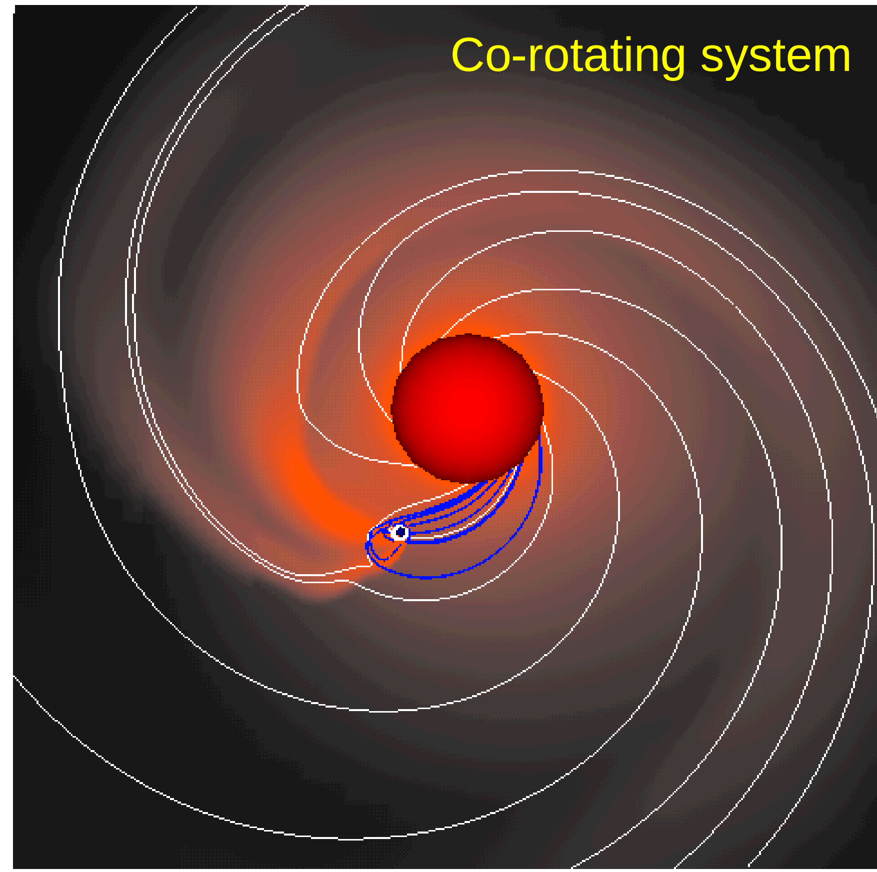

High mass X-ray binaries (HMXRB)

Fast winds (1500 – 4500 km/s)
Large mass-loss: ~ 10^{-5} $M_{\odot}$/y (WR)
10^{-6} - 10^{-8} $M_{\odot}$/y (OB-stars)

Symbiotic binaries
(Red Giant + White Dwarf)

Slow winds (10 – 60 km/s)
Large mass-loss: ~ 10^{-6} - 10^{-10} $M_{\odot}$/y

Micro-quasars: systems with jets

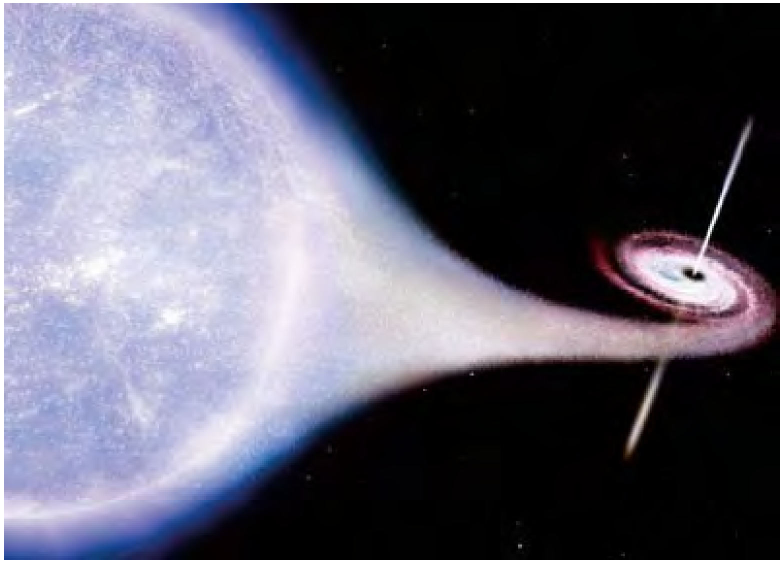

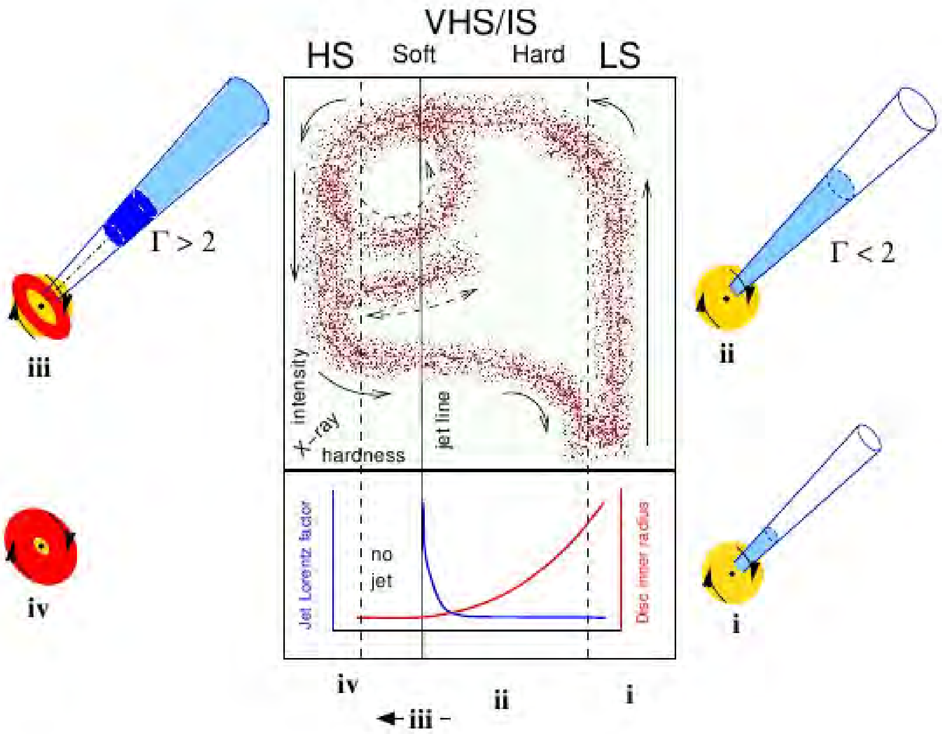

Paradigms:
Disk-jet systems, RLO

Fender et al. Ann. Rev. AA. 42, 317 (2004)

Wind-accreting high mass systems (e.g. Cyg X-1) do not really fit into the scheme

- no switch-off state (persistent X-ray emission)
- non-thermal emission contributes always significantly
- jets in states with relative large thermal emission only (Fender et al. 2006)?
- In Cyg X-1 dark jets bow-shocks (Tudose et al. 2006; Russell et al.2007) or background SNR (King et al. 2012).

Multi-scale simulation
of high-mass microquasars
(at the example of Cyg X-1)

Cygnus X-1

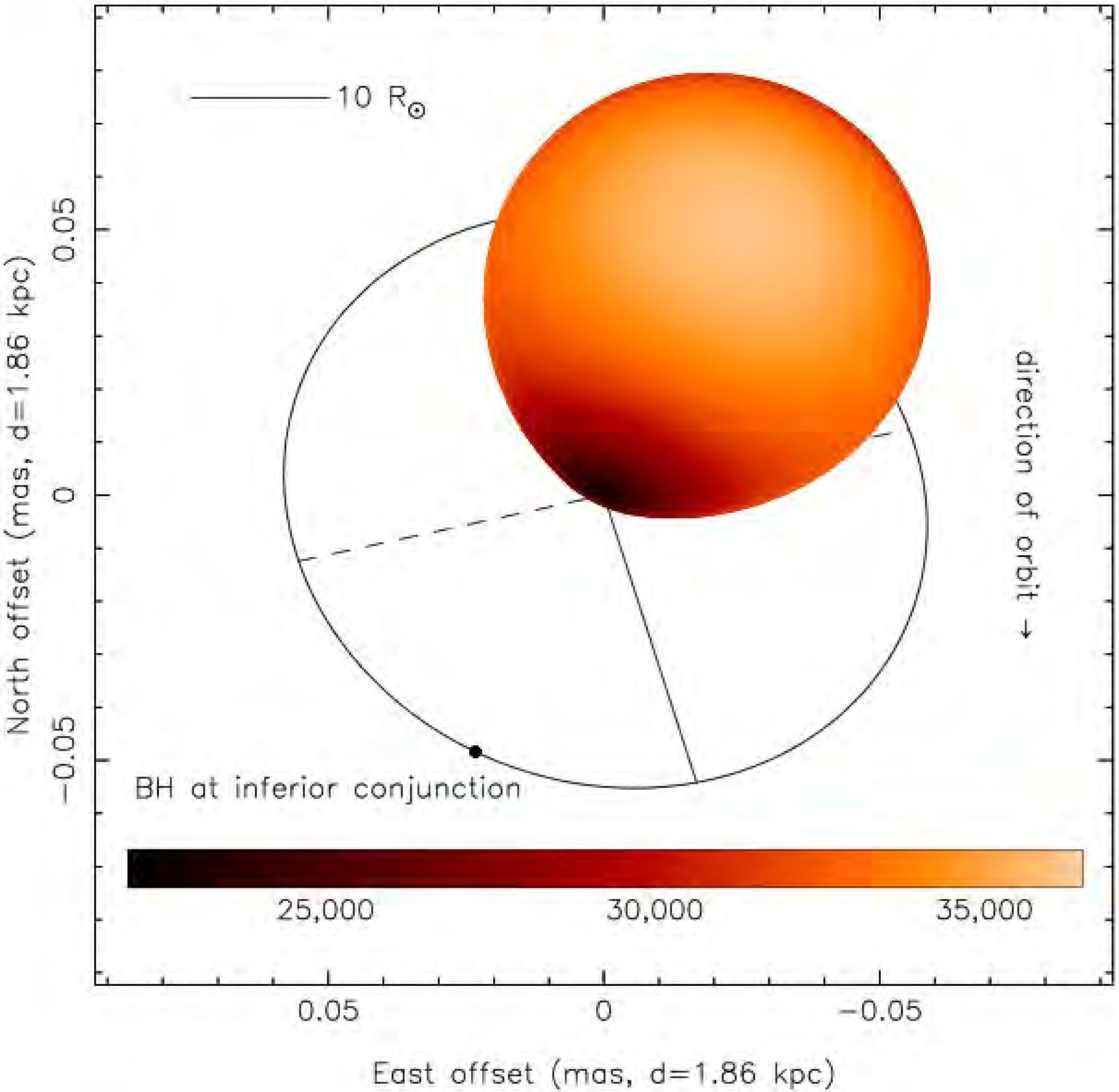

parameter	value
i (deg)	27.06 ± 0.76
Ω	1.400 ± 0.084
e	0.018 ± 0.003
ω (deg)	307.6 ± 5.3
M_{opt} ($M_\odot$)	19.16 ± 1.90
R_{opt} ($R_\odot$)	16.17 ± 0.68
$\log g$ (cgs)	3.303 ± 0.018
M ($M_\odot$)	14.81 ± 0.98

P = 5.599829 ± 0.000016 days
a = $2.99\ 10^{12}$ cm = 42.96 $R_\odot$
R_{opt}/a = 0.3765

$q = M_{BH}/M_{opt}$ = 0.773
$R_{Roche,\ equiv.}$ = 0.415/a = 1.1 R_{opt}

Orosz et al., ApJ 742, 84O, 2011

Line driven winds

Massloss is driven by scattering of UV-photons in some 10^7 lines

Temperature and ionization structure in wind determines which lines are active

One can show (CAK: Castor, Abott, and Klein theory) :

1) $v_\infty \sim 2.6\ v_{esc}$ (T* > 21'000 K; Lamers et al. 1995)
Note that v_{esc} depends on luminosity and temperature
since is corrected by the continuum force:
Thompson scattering of photons on free electrons.

2) $v(r) = v_\infty\ (1 - R^*/r)^{0.8}$ (for MS O-stars; Lamers & Cassinelli 1999)

3) Massloss rate is given by luminosity.

For the present study, we decided on isotropic winds (in the rest frame of the star) and on a parameter study of different wind speeds

v_W = 750, 850, 1000, 1500, 2000, 2500 km/s

Note 2500 km/s is certainly to high for Cyg X-1, but will extend the parameter study

Hydrodynamical simulations, Eulerian frame of reference with the stars moving within the computational domain 10 (19) levels of refinement

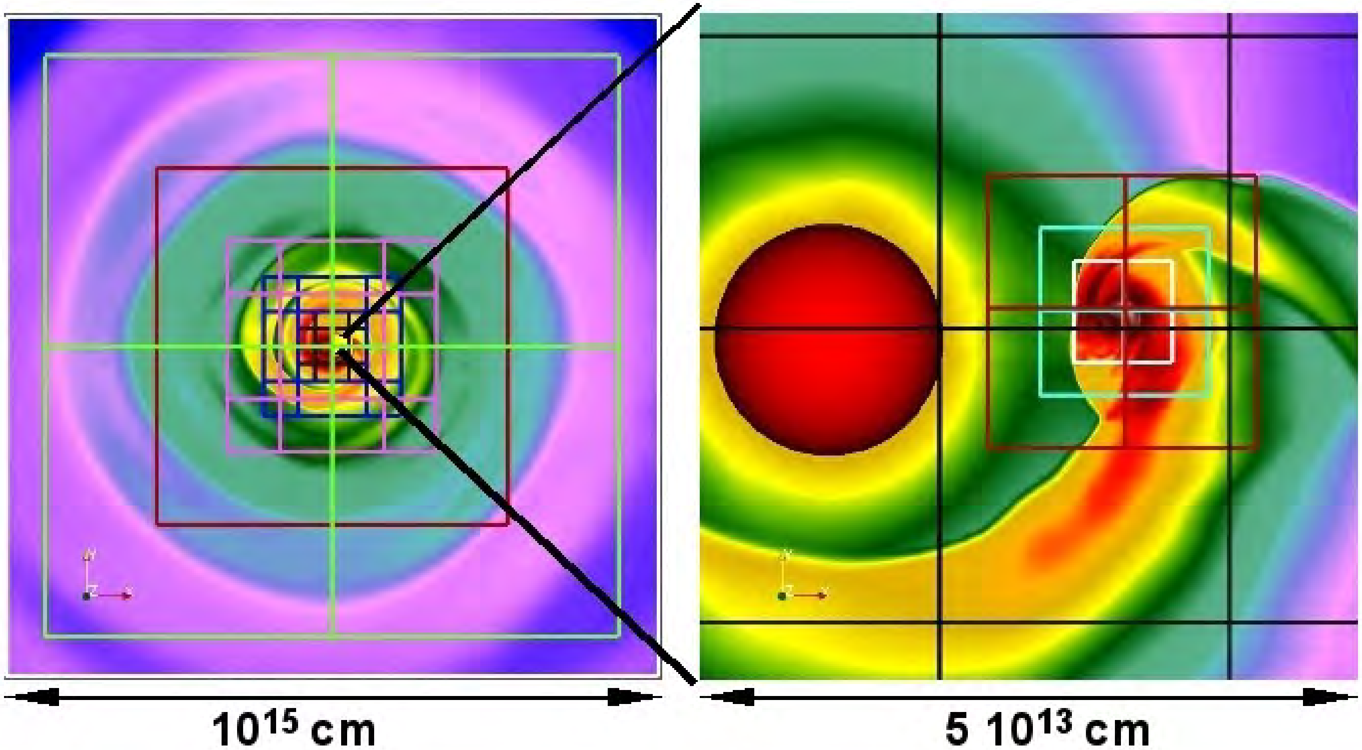

- ➔ From one level to the next, grid cells are refined by a factor of two.
- ➔ Levels 1-6 are fixed in space, levels 7 to 10 (19) move with the CO.
- ➔ Each level comprises between 8 and 256 individual grids
- ➔ The entire mesh consists of 256 – 1024 grids and 10^7 – 10^{10} cells
  (Note: this would consist of ~ 10^{20} cells on a uniform mesh !!!)

The decomposed grid structure is exploited for parallelization

Simulations are carried out in an Eulerian frame of reference with the stars moving within the computational domain 10 (19) levels of refinement

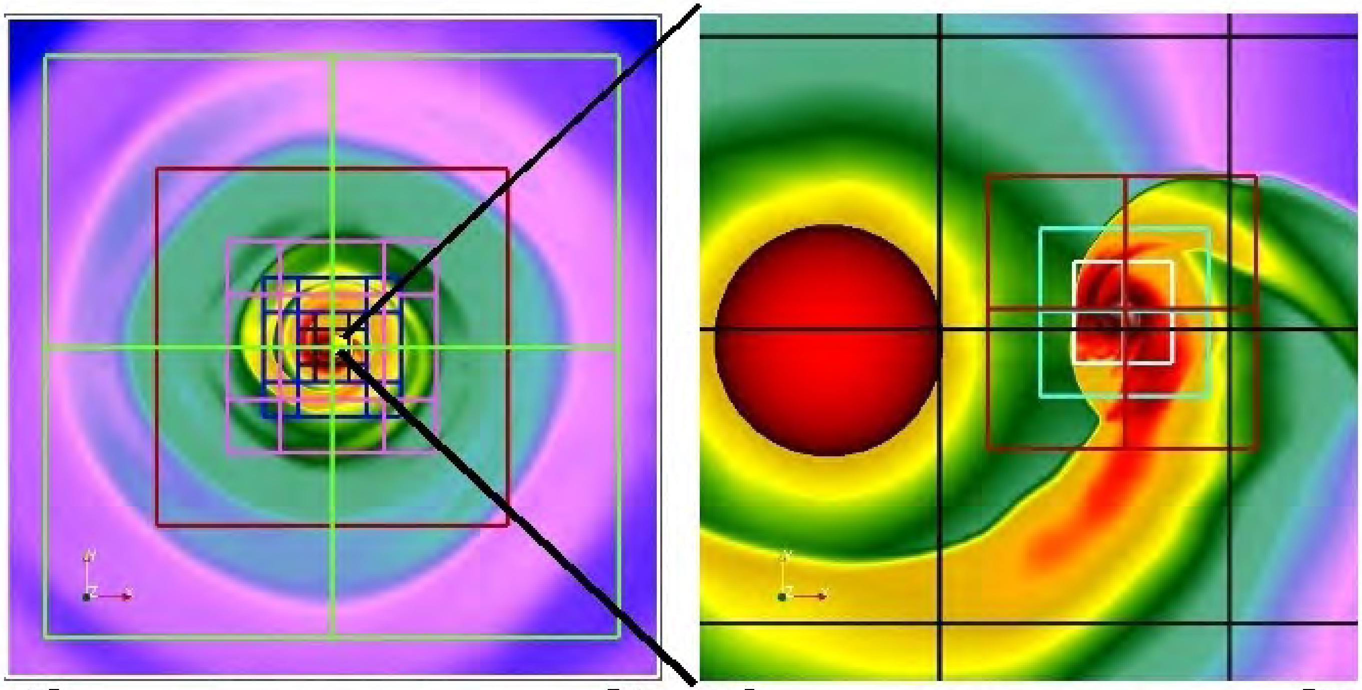

- ➔ Basic domain discretization: $\Delta x = 10^{13}$ cm (~ 1/3 AU, ~ 3 a_S) Δt~ 30 s
- ➔ Orbital scale (~1 AU): Δx= 3.125 · 10^{10} cm (~ 1/300 a_S, ~ 1/36 R_O) Δt~1s
- ➔ BHL scale (10^{10} – 10^{11} cm) : Δx= 10^8 – 10^9 cm Δt~1/100 s
- ➔ Accretor scale, 37 (RG = M/c^2) ~ 10^7 cm : Δx= 2.5 10^6 cm Δt= 0.1 ms

Large scale structure of a wind-accreting system

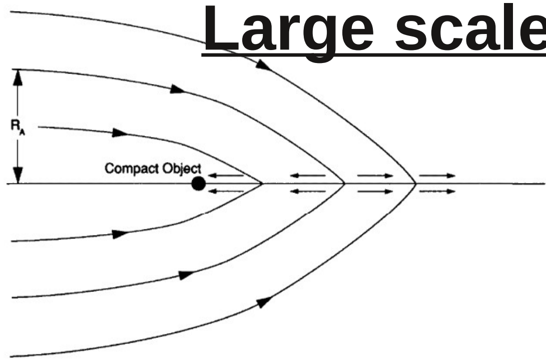

Accretionline of Bondi-Hoyle-Lyttleton-theory expands into a wake

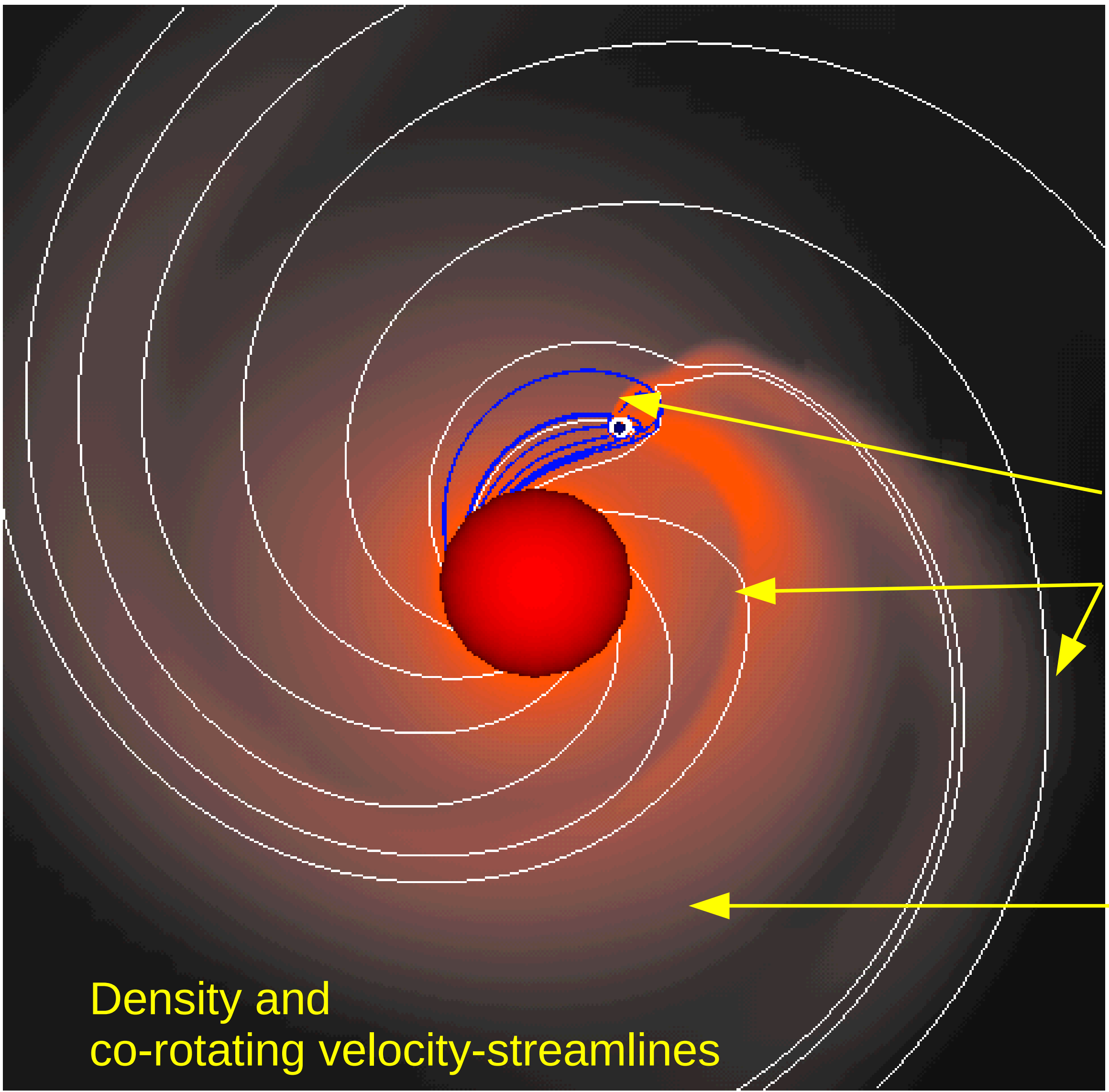

1) The wake is spirally shaped, do to the movement of the accretor through the medium.
   To first order, this is an Archimedian spiral with an opening angle given by the ratio of orbital to wind velocity.
   Similarity to colliding wind binaries (RW 1995).

2) At the tip of the wake is a bow-shock.

3) It gradually converts to a slip plane.

Excretion part of the wake

Large scale structure of a wind-accreting system

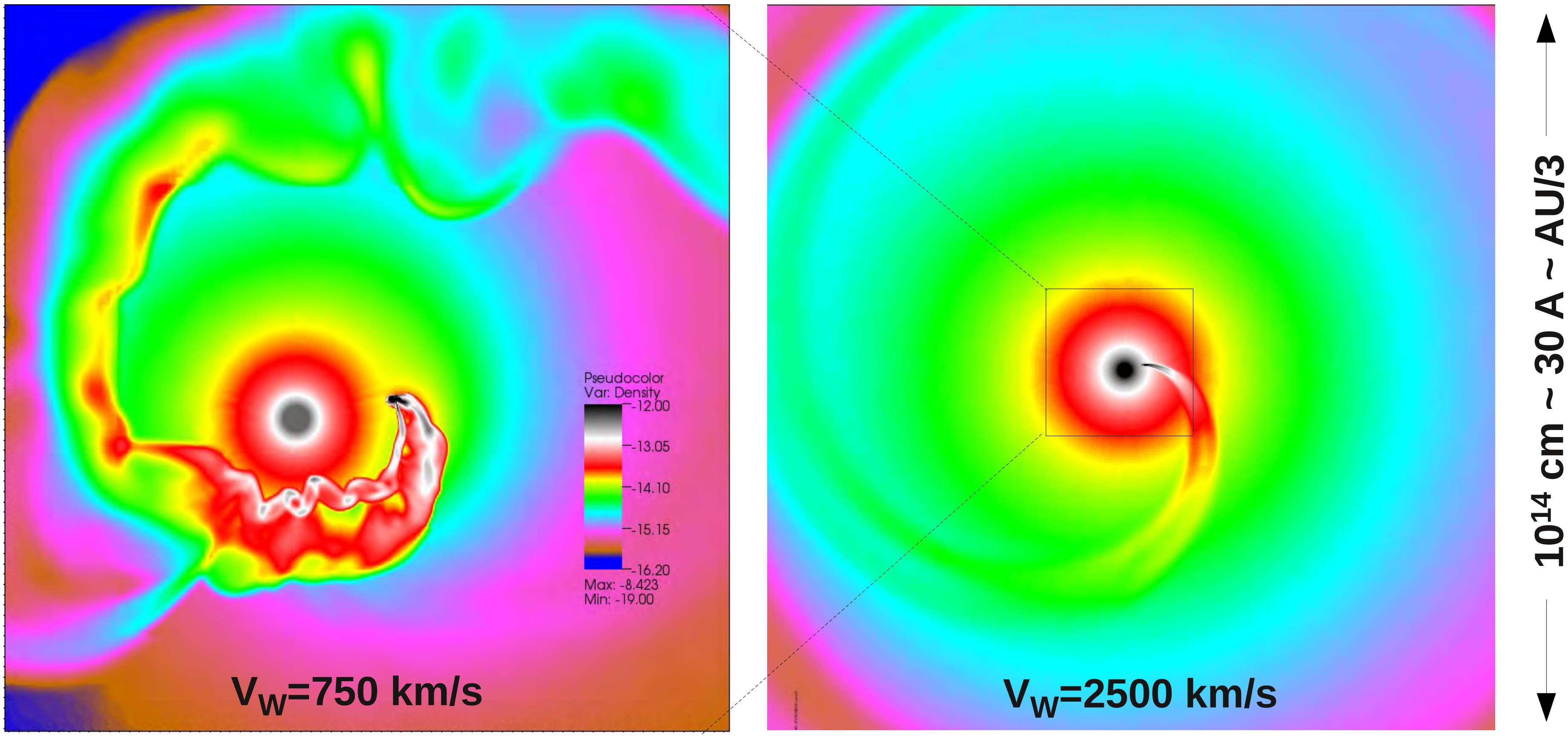

Note: if not otherwise stated, all graphs show density.

Formation of accretion wake shock (v_w = 2500 km/s)

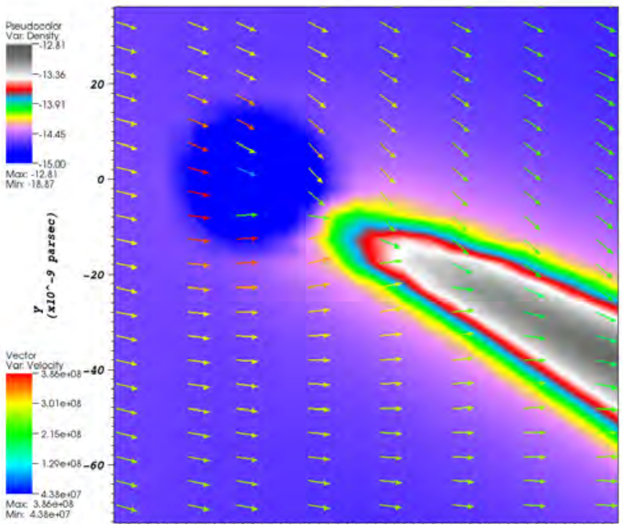

R_B = 20'000 R_G

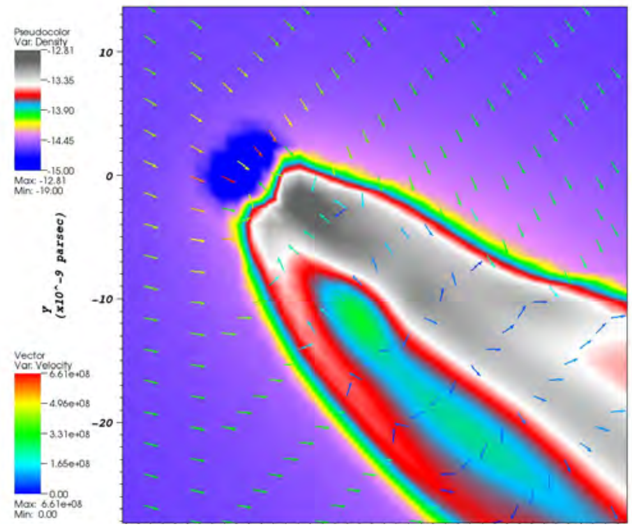

R_B = 5'000 R_G

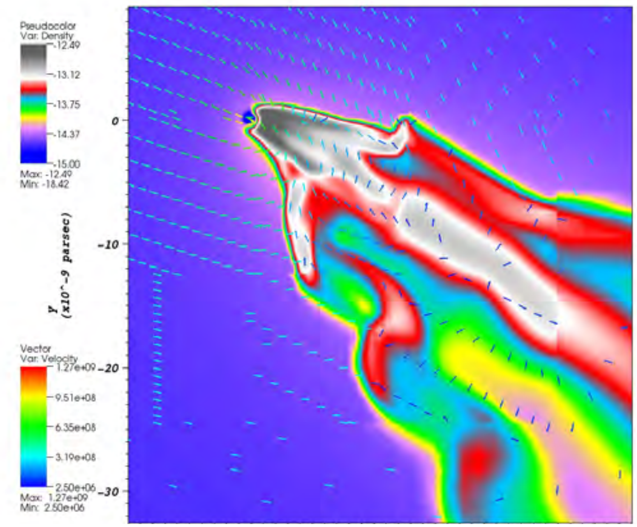

R_B = 1'250 R_G

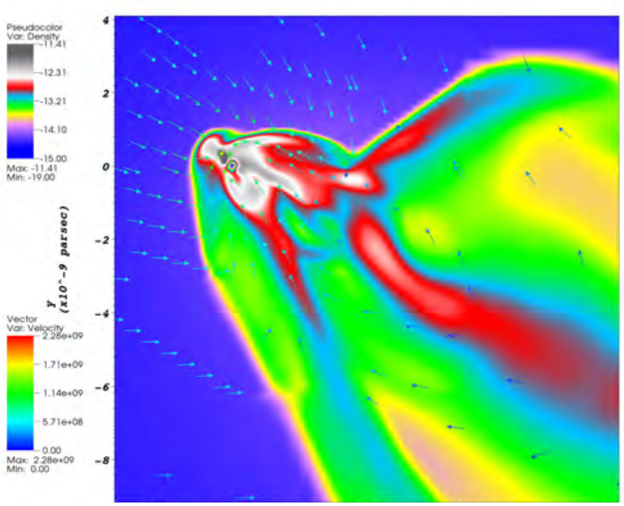

R_B = 300 R_G

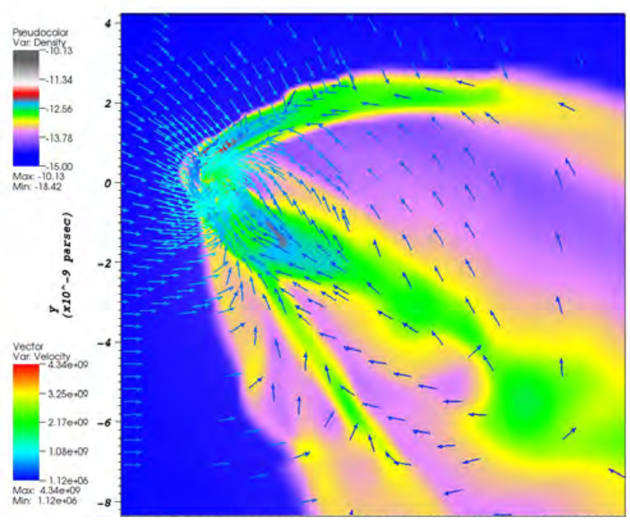

R_B = 75 R_G

R_G : Schwarzschild radius

$R_G = 2GM/c^2$

R_B : Radius of boundary

$\Delta x \sim R_B/6$

Necessary resolution to couple accretion flow around compact object and large scale flow: ~ 300-500 Schwarzschild radii

BHL-Accretion rate

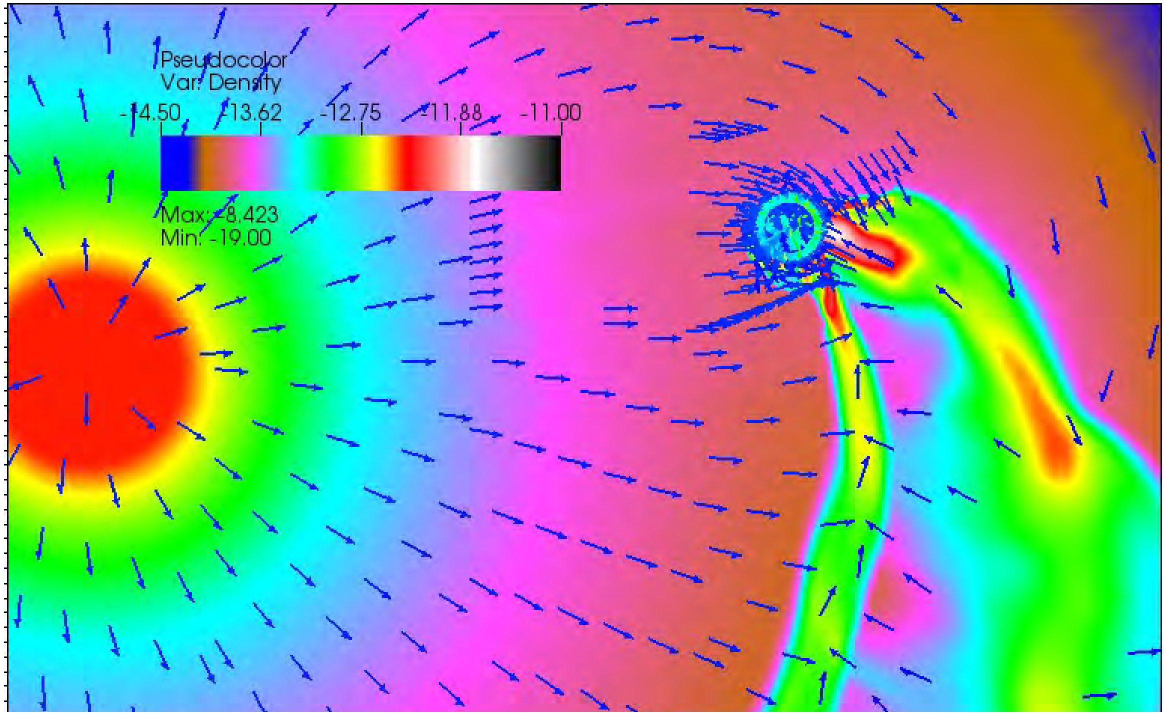

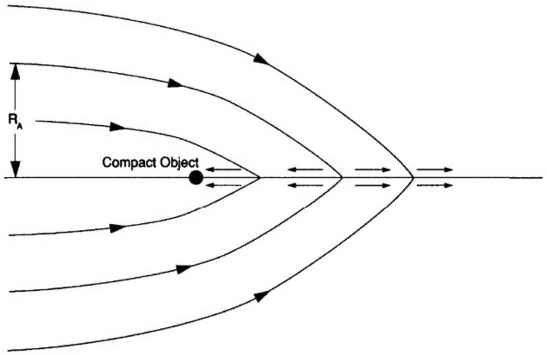

Bondi-Hoyle picture

$$\dot{M}_{HL} = \frac{4\pi\,(GM)^2\,\rho_\infty}{V_\infty^3} = M_{ML}\frac{(GM)^2}{V_\infty^2}$$

In reality:
- diverging flow
- no accretion line
- accretion wake tilted against accretion flow

Nevertheless: BHL-theory predicts about the correct value for mass accretion!

BHL-Accretion rate

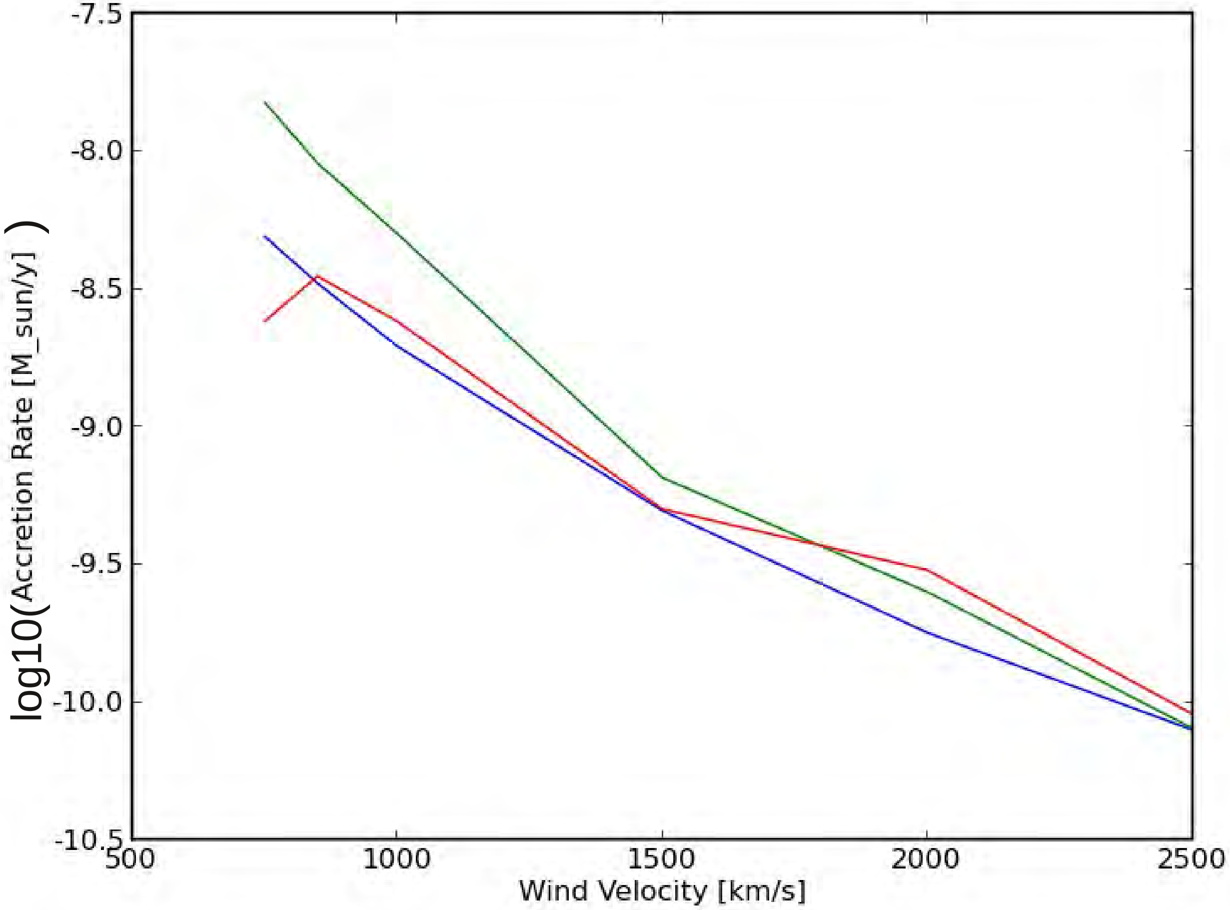

Bondi-Hoyle-Lyttleton accretion rate

Measured accretion rate (g=5/3)

Measured accretion rate (g=1.1)

BHL-Accretion rate

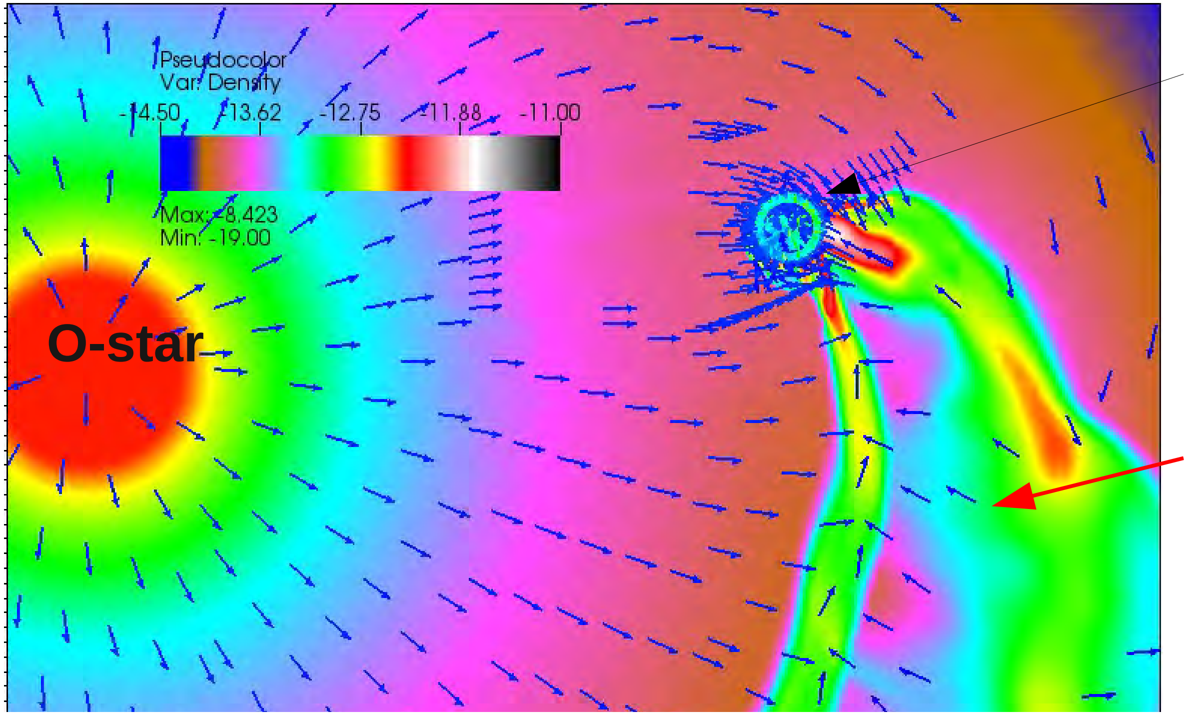

About all material which flows through the BHL-accretion cylinder finally will be accreted

→ **BHL-theory predicts about the correct value for mass accretion!**

But: wind material moves ballistically. By this, most of the material passes through the accretion wake on its way down into the BH.

→ Dissipation of energy and angular momentum on the bounding shocks !
BHL-theory does **NOT** predict the correct amount of accreted angular momentum!

Accretion shock position

(with respect to the BH)

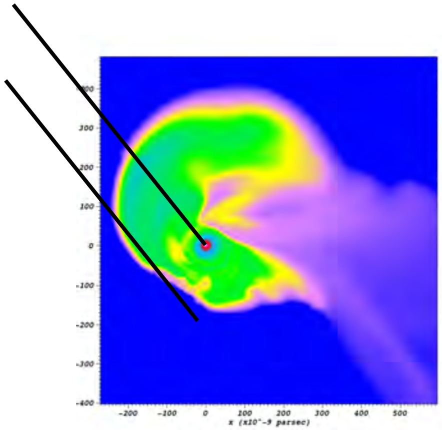

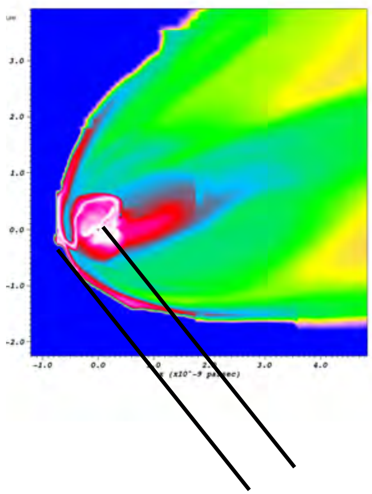

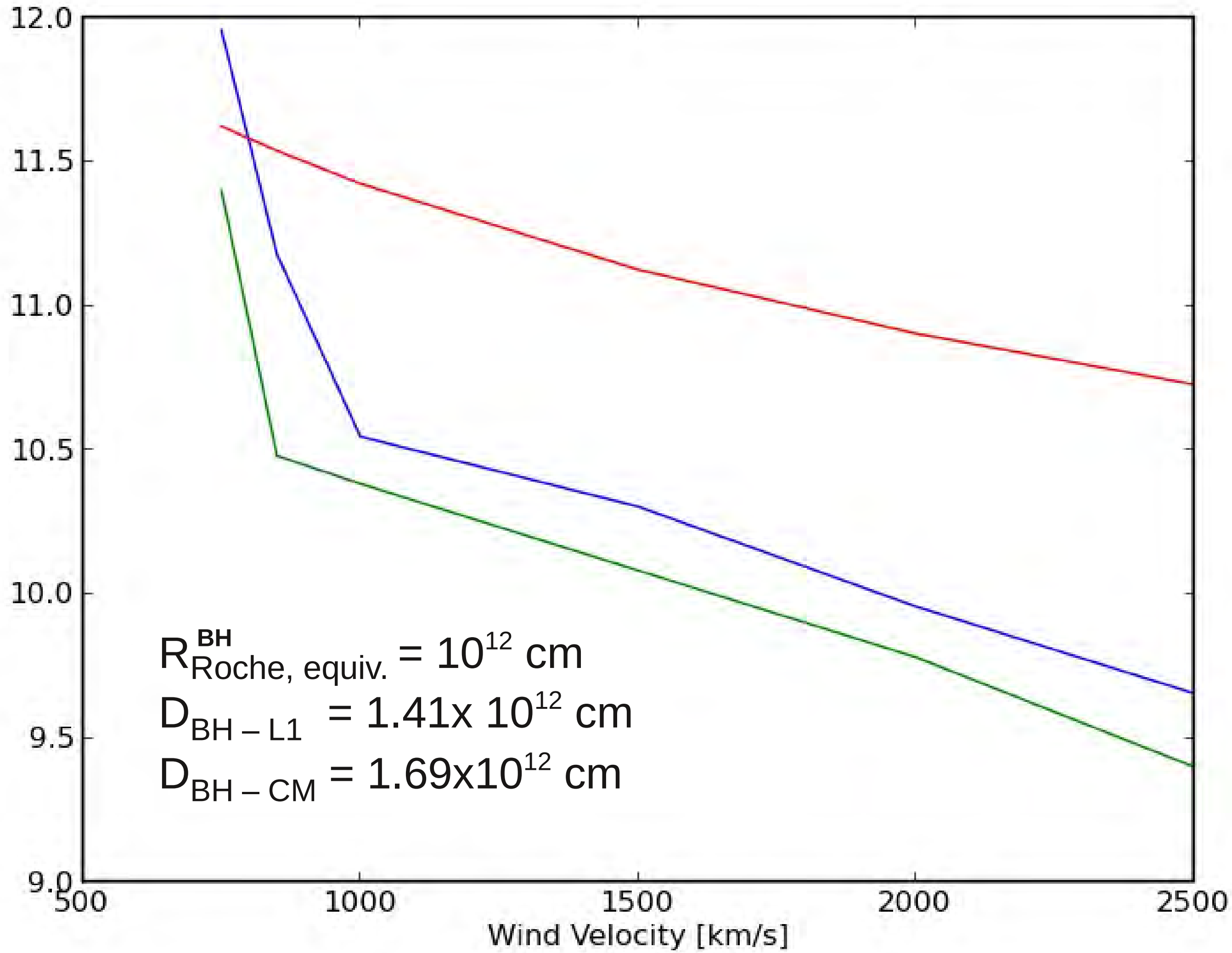

- Red line: Bondi-Hoyle-Lyttleton accretion radius : $2GM_{BH}/(v_W+v_O)^2 \sim 2GM_{BH}/(v_W)^2$
- Blue line: Measured shock radius (g=5/3)
- Green line: Measured shock radius (g=1.1)

Accretion shock position

(with respect to the BH)

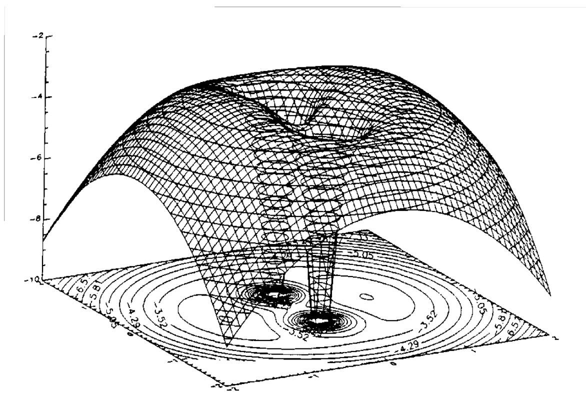

If region of shocked material is deep in the well:

something different is going to happen

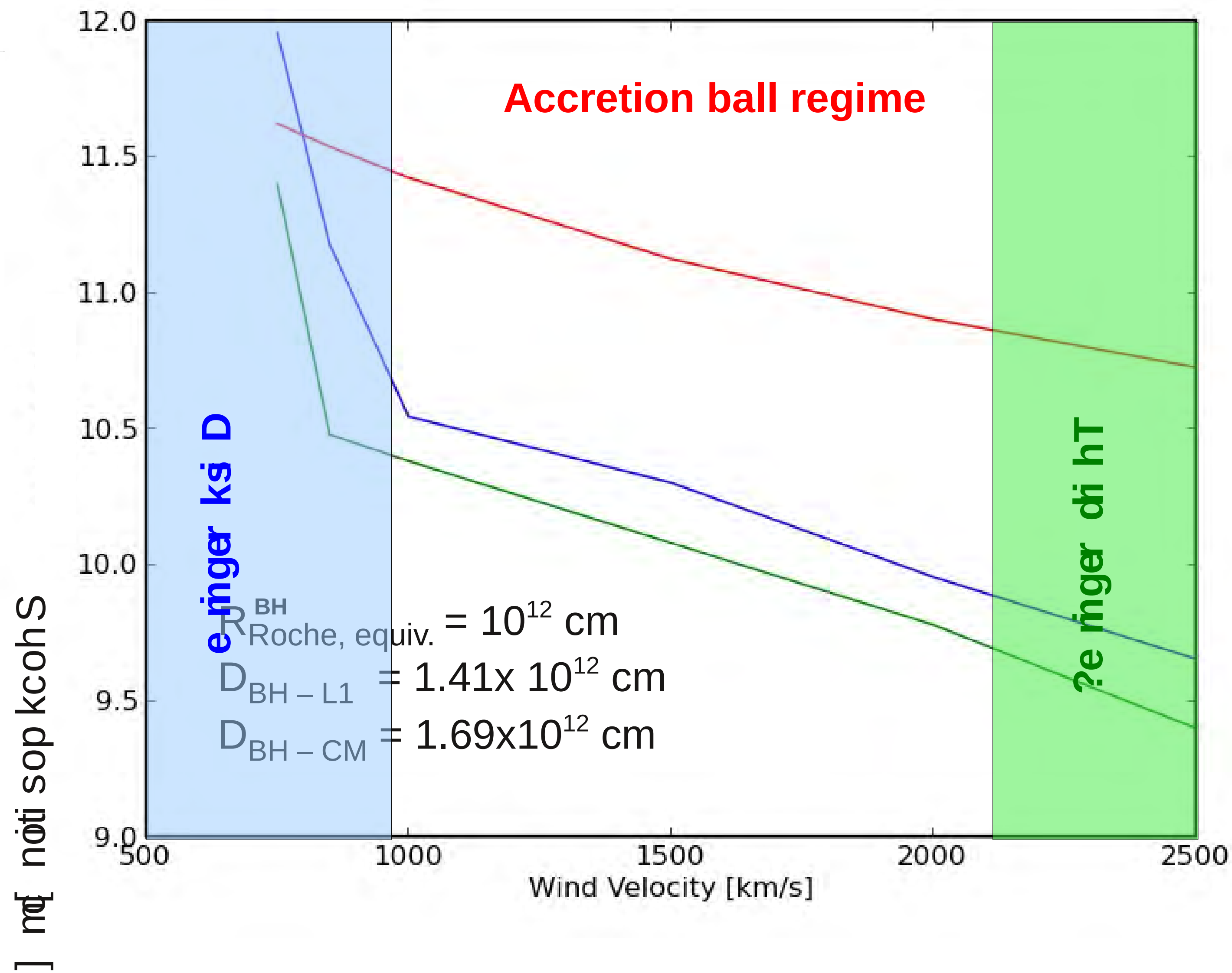

Bondi-Hoyle-Lyttleton accretion radius : $2GM_{BH}/(v_W+v_O)^2 \sim 2GM_{BH}/(v_W)^2$

Measured shock radius (g=5/3)

Measured shock radius (g=1.1)

The disk regime (v_w < 900 km/s)

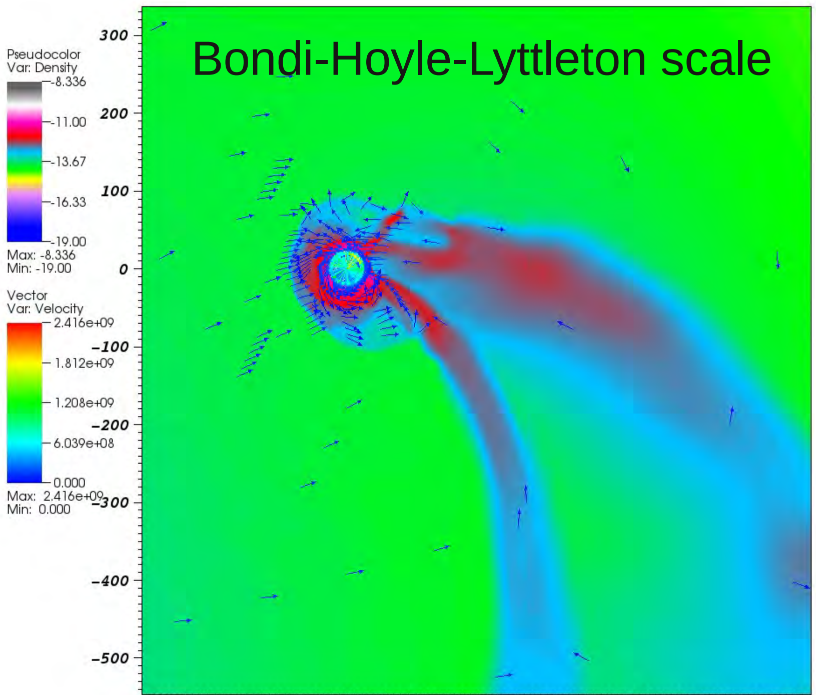

Courtyard scale (for v_w = 750 km/s
~ $R_{BHL}/5$ ~ 2000 R_G

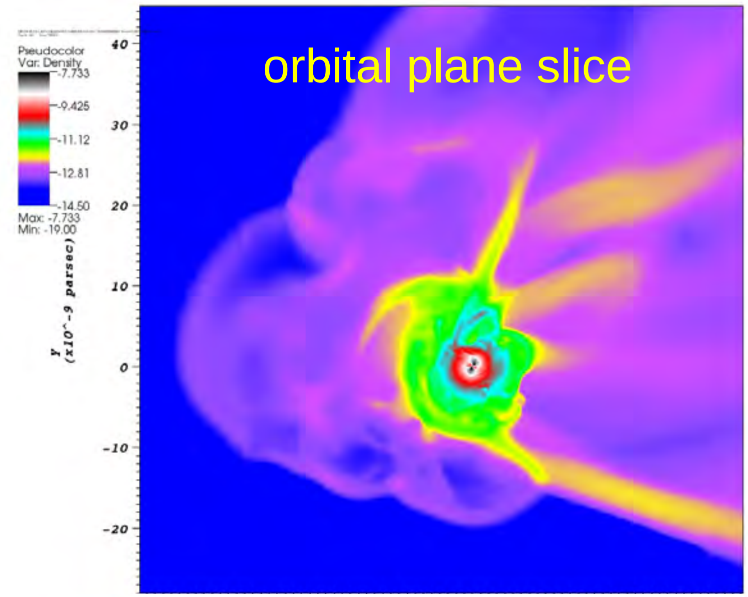

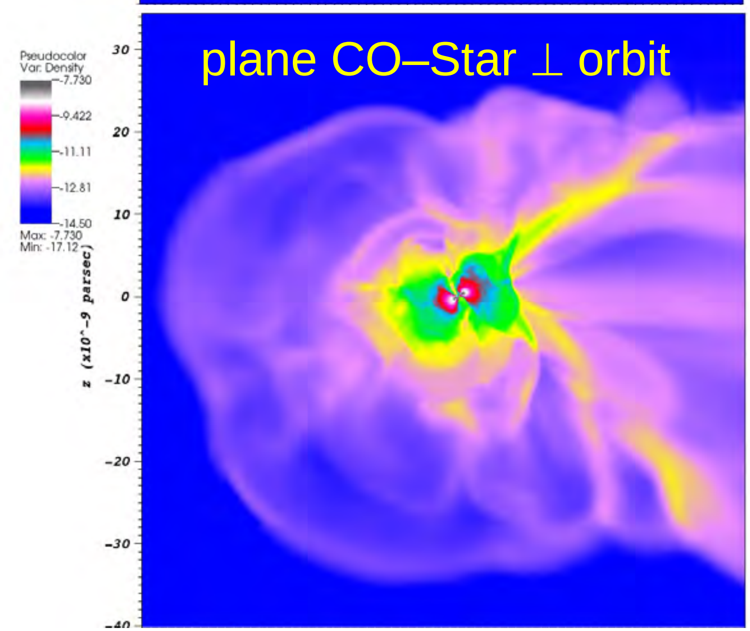

Bow shock gives courtyard-scale.

Spinning structure has size of ~ 1/3 of courtyard

The disk regime (v_w < 900 km/s)

Courtyard scale (for v_w = 750 km/s
~ $R_{BHL}/5$ ~ 2000 R_G

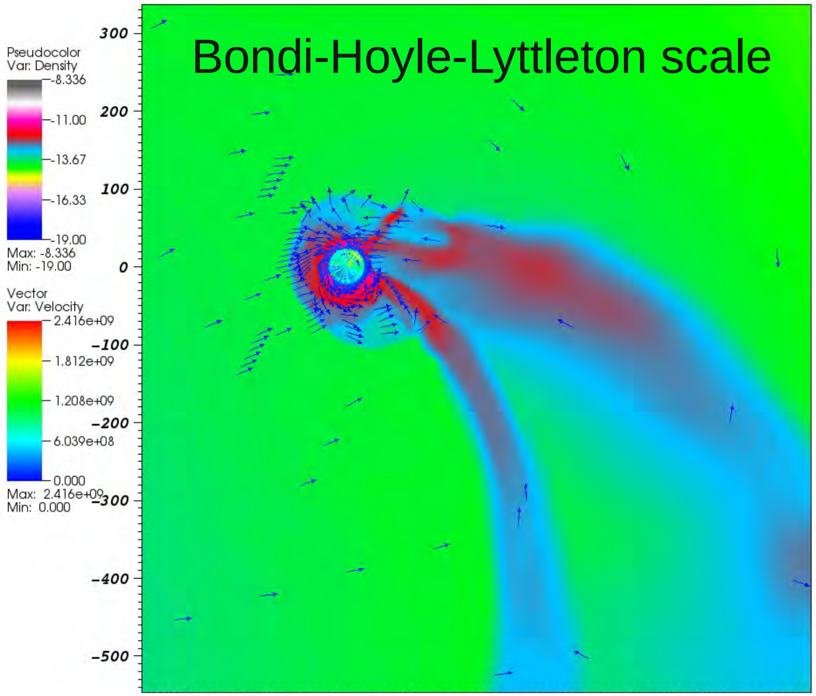

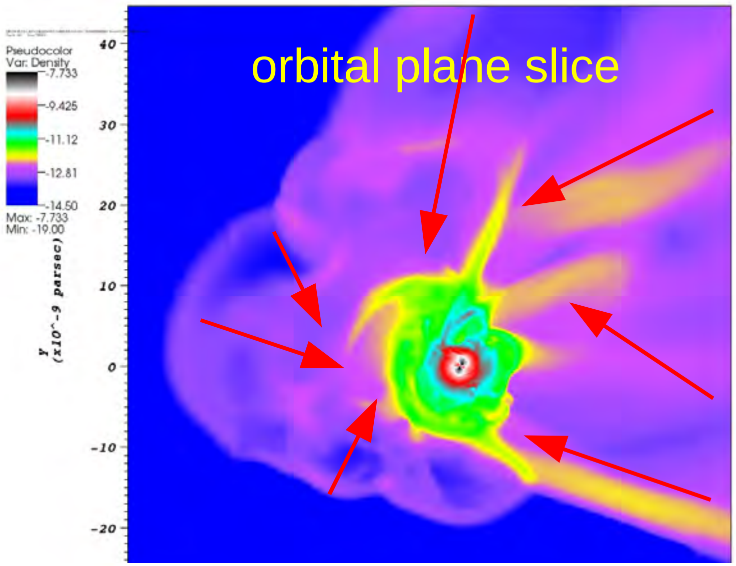

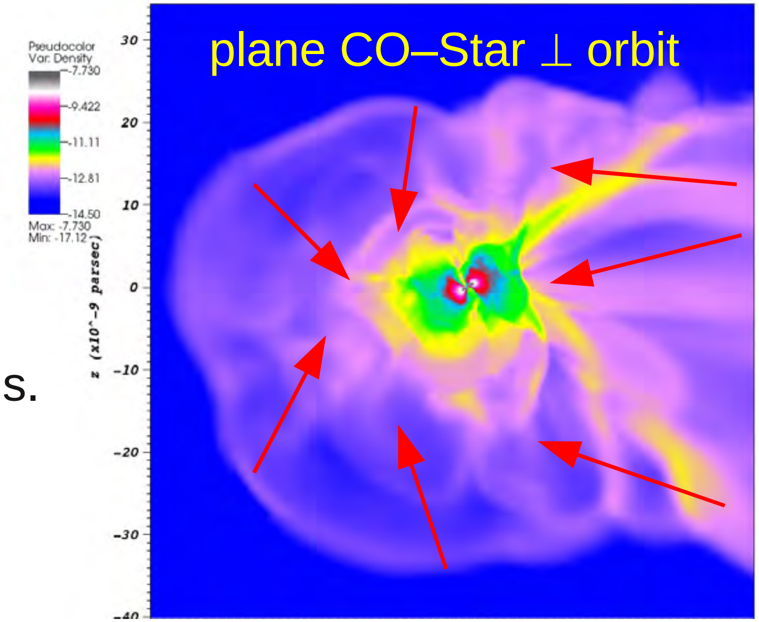

On the courtyard-scale, different streams originating from the BHL-wake collide amongst them-selves and the spinning structure.

→

Supersonic turbulence develops in the courtyard
Flat density-profile with order of magnitude fluctuations.

Strong outward moving waves are generated.

→ **MOVIE**

Analysis of planar supersonically colliding flows:

Folini & Walder (2006); Folini, Walder, & Favre (2013 submitted)

“oblique shocks force turbulence ↔ turbulence forces shocks to be oblique”

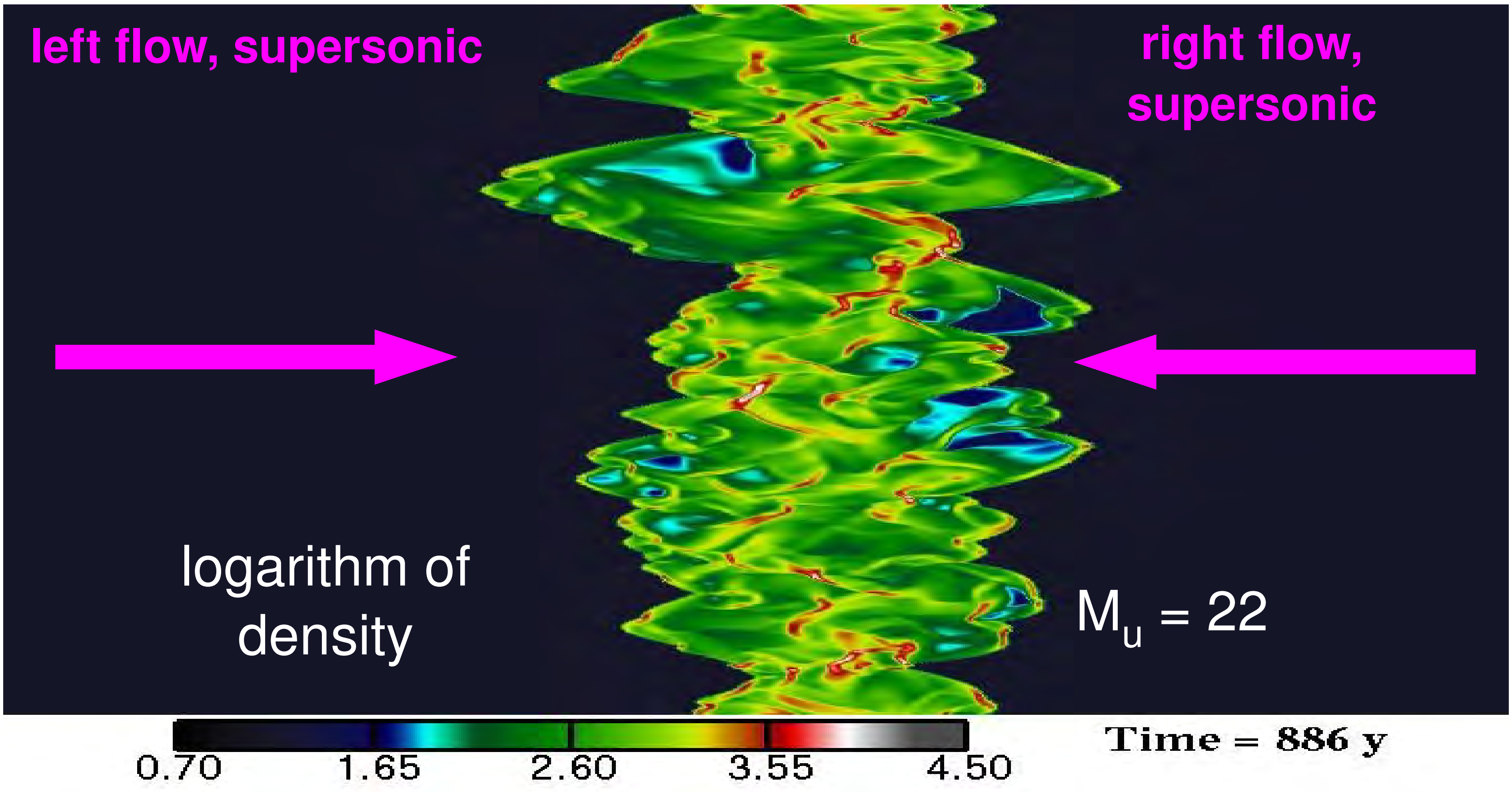

Analysis of planar supersonically colliding flows:

Folini & Walder (2006); Folini, Walder, & Favre (2013 submitted)

"oblique shocks force turbulence ↔ turbulence forces shocks to be oblique"

1) Forcing scale given by slab thickness
2) Forcing compressible and solenoidal
3) Turbulence strongly anisotropic

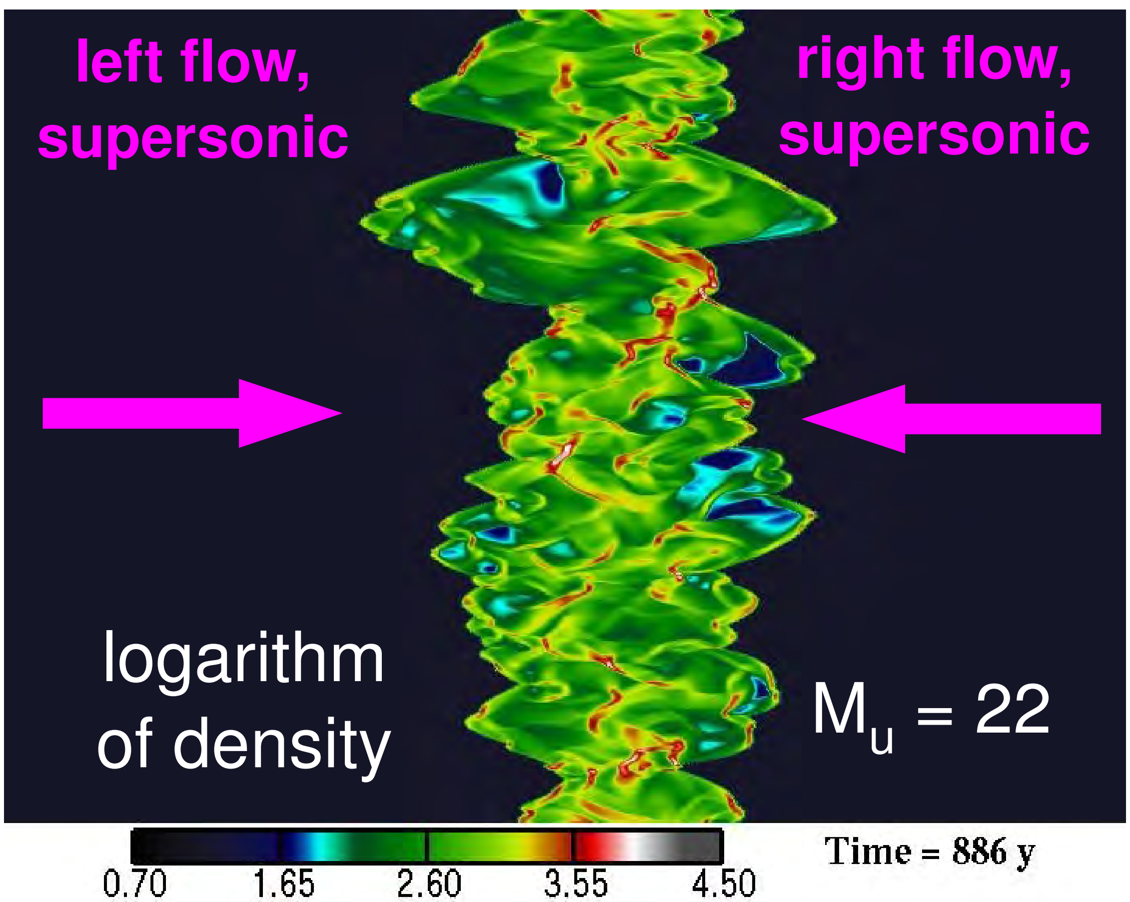

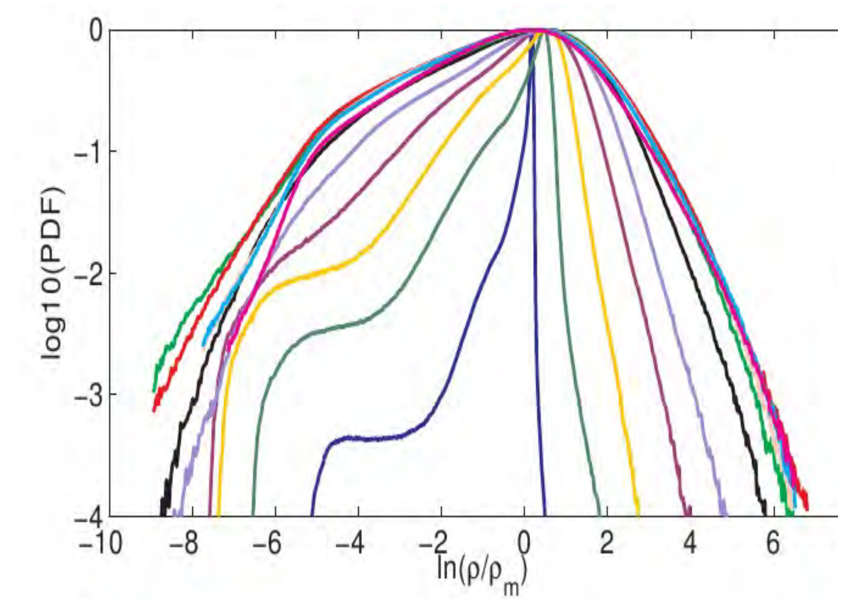

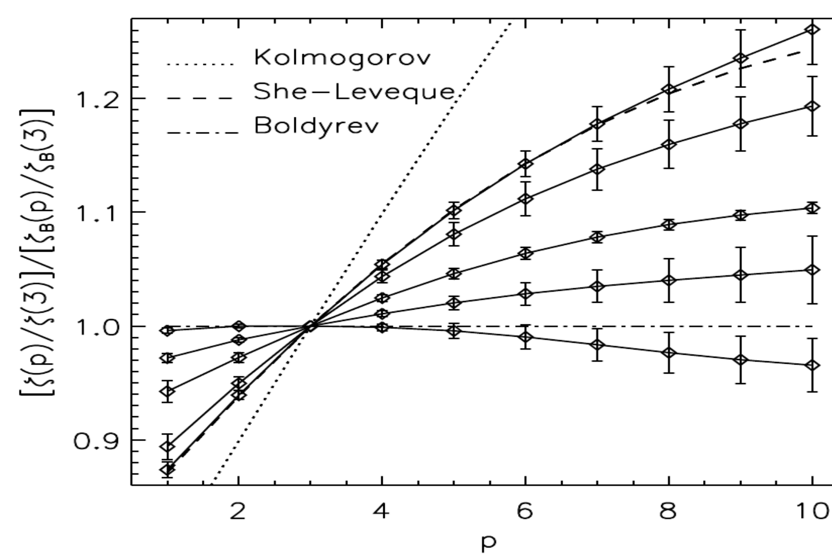

How the disk finally forms

In the wake, the flow field is highly supersonically turbulent:

Supersonic flow moves close to ballistically in the gravitational field of the BH.

However, as different streams start from different locations in different directions, they collide: strong shocks form.

Each shock passage dissipates energy and angular momentum.

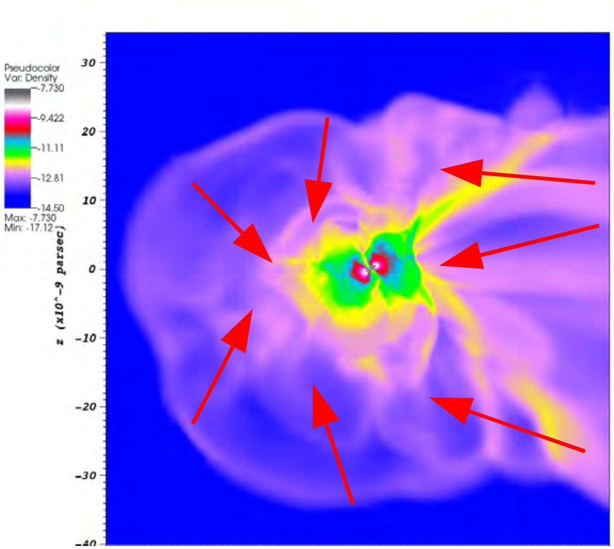

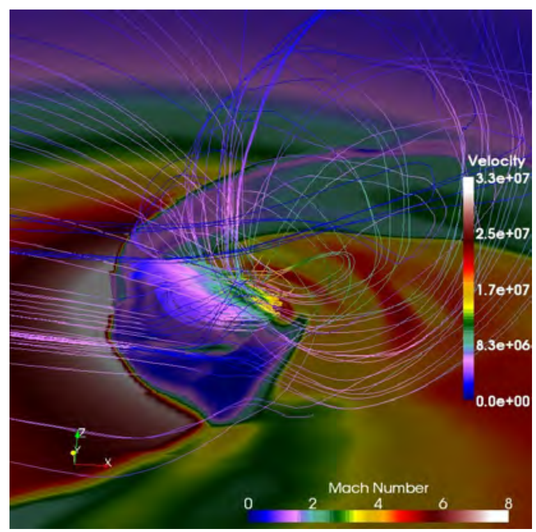

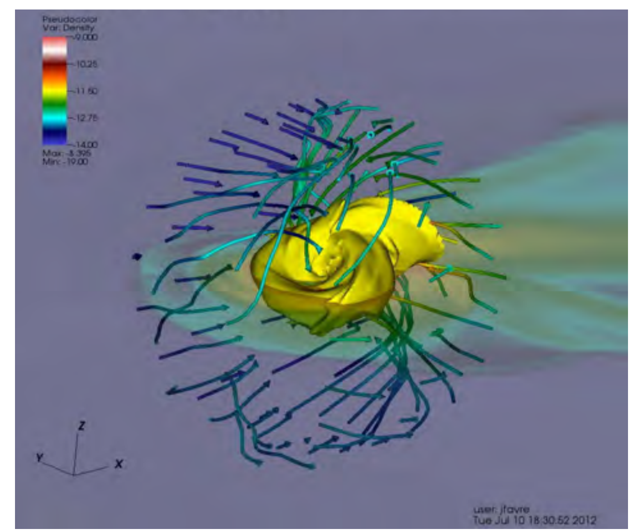

The different streams

3D flow structure

Qualitative, heuristic analysis on the basis of graphs.

Quantitative analysis yet to come,
but should go along what was done in planar colliding flows

How the disk finally forms

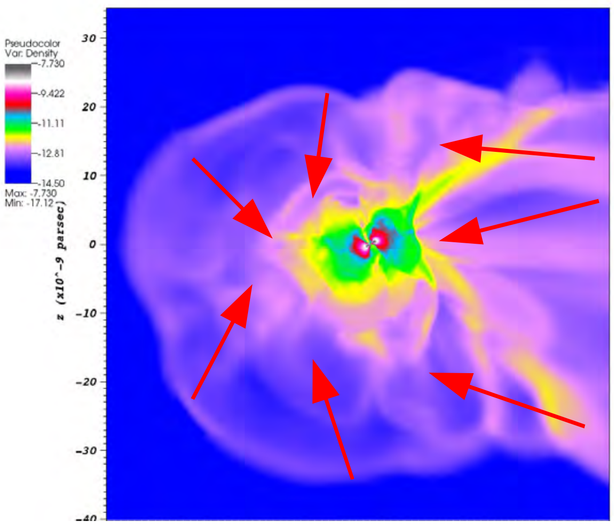

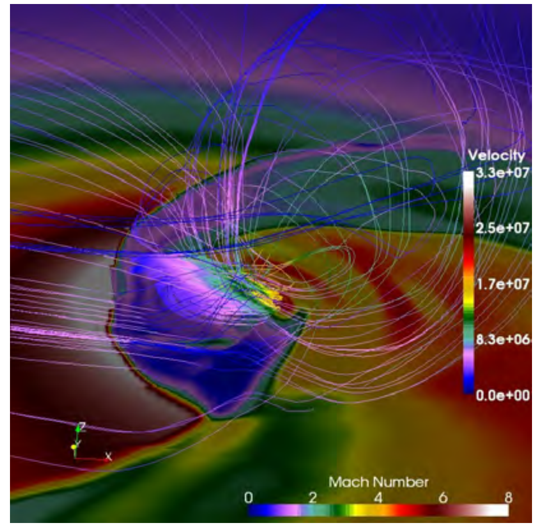

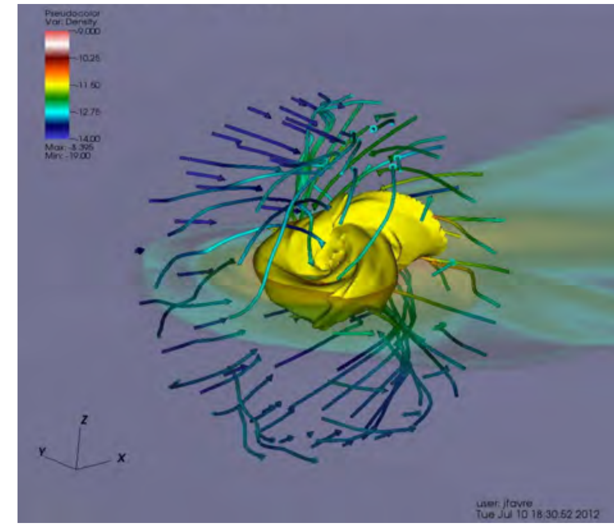

The different streams

3D flow structure

Spherical slice at different radii, showing:

- density (semitransparent)
- velocity field
- arrows out of the ball indicate velocities outwards
- shadowed arrows within the ball: velocities inwards

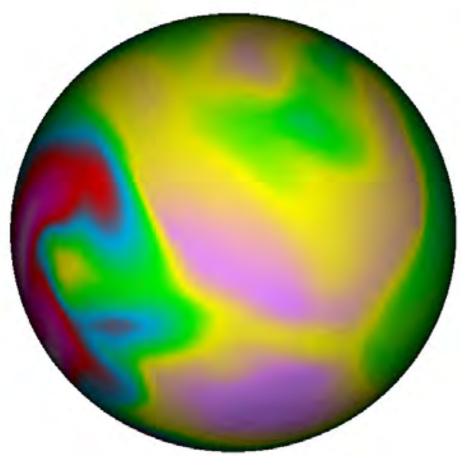

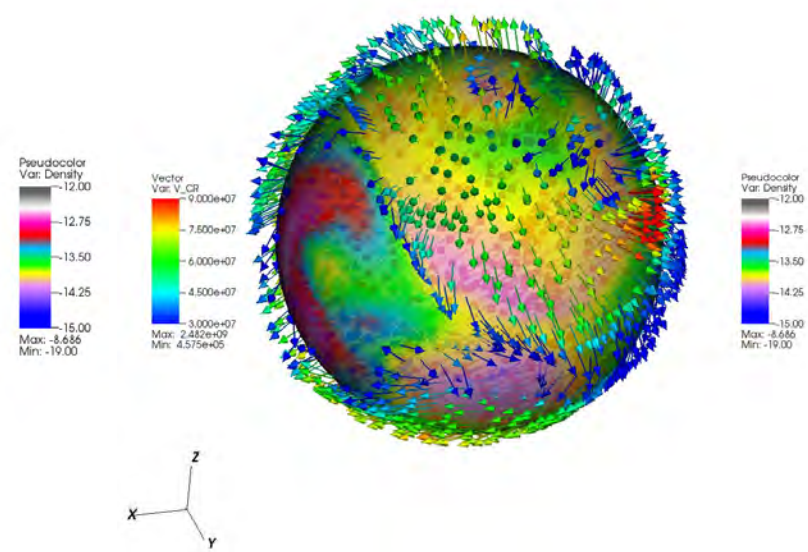

Disk-formation by dissipation of energy/angular momentum in shocks

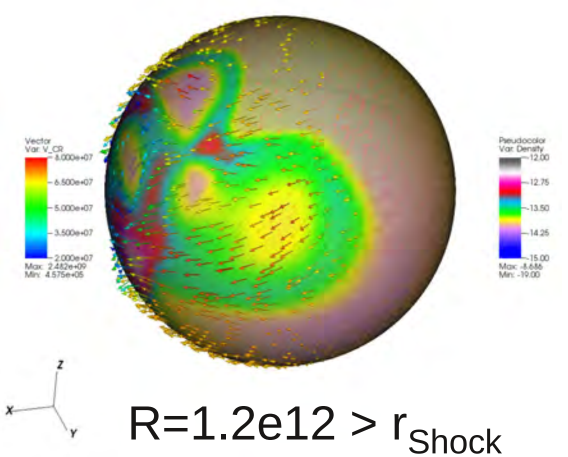

R=1.2e12 > r_{Shock}

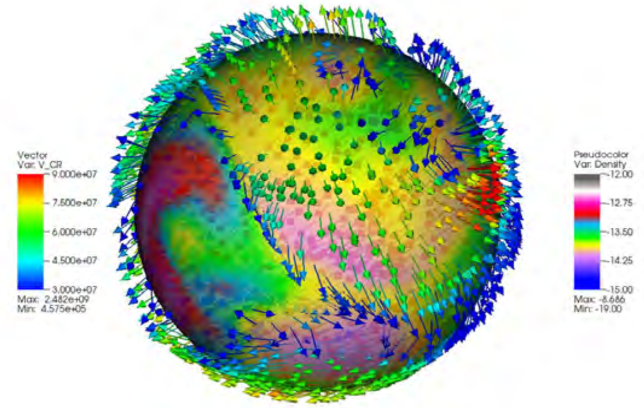

R=6e11 ~ r_{Shock}

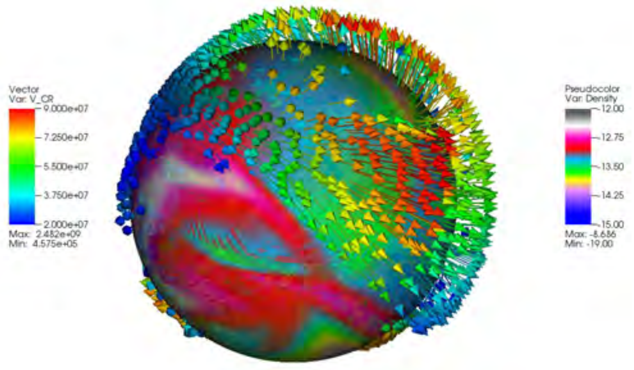

R=3e11 < r_{Shock}

Disk-formation by dissipation of energy/angular momentum in shocks

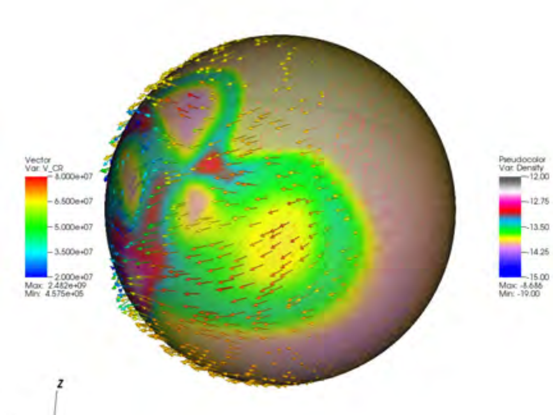

R=1.2e12 > r_{Shock}

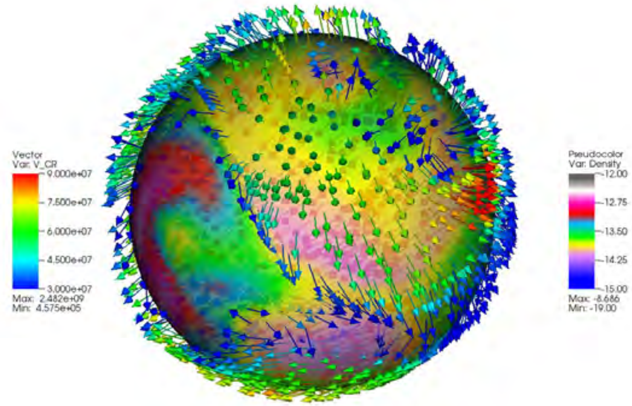

R=6e11 ~ r_{Shock}

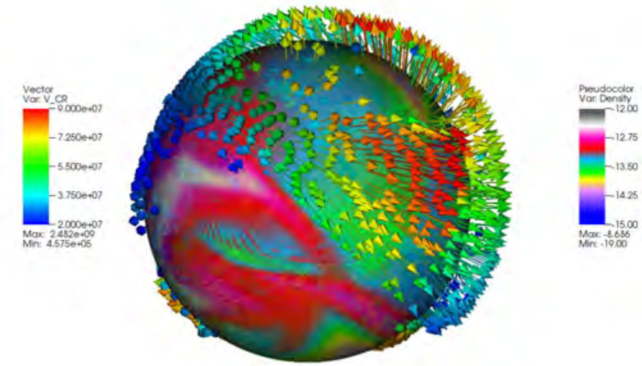

R=3e11 < r_{Shock}

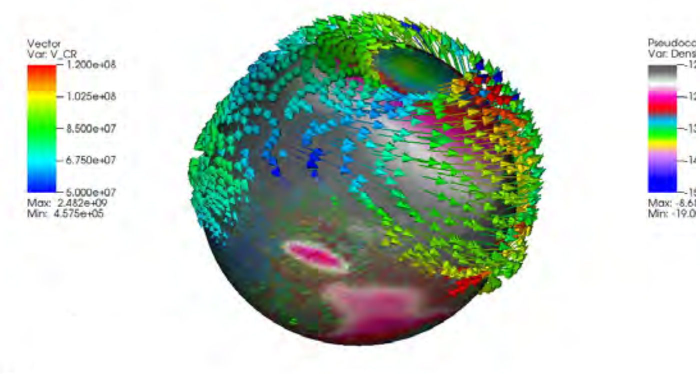

R=1.5e11

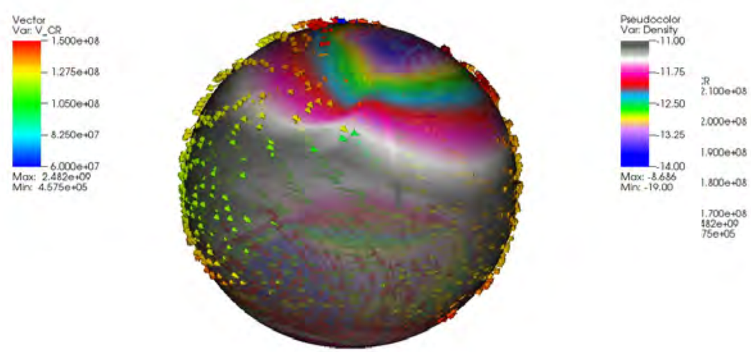

R=7.5e10

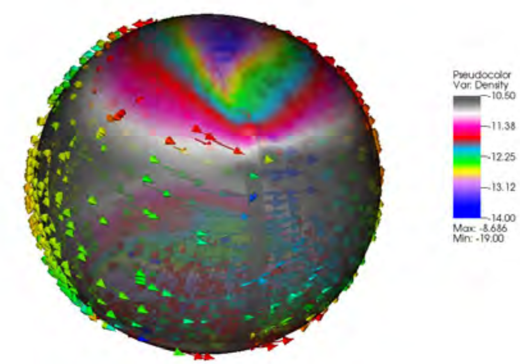

R=3e10

Disk-formation by dissipation of energy/angular momentum in shocks

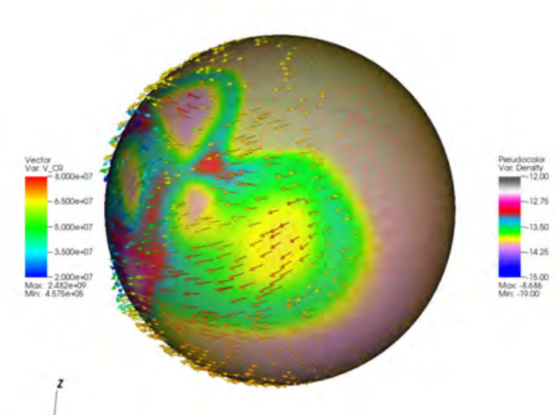

R=1.2e12 > r_{Shock}

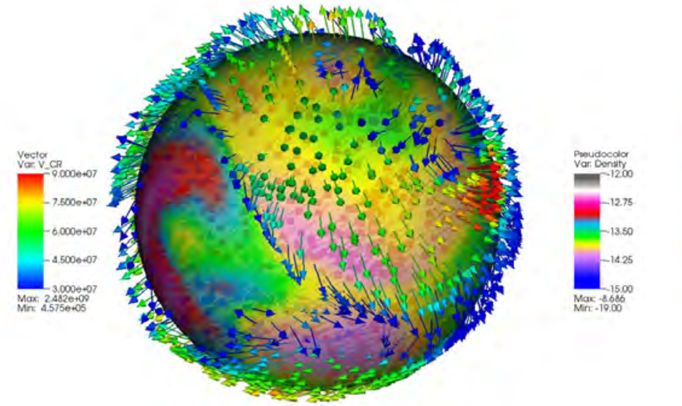

R=6e11 ~ r_{Shock}

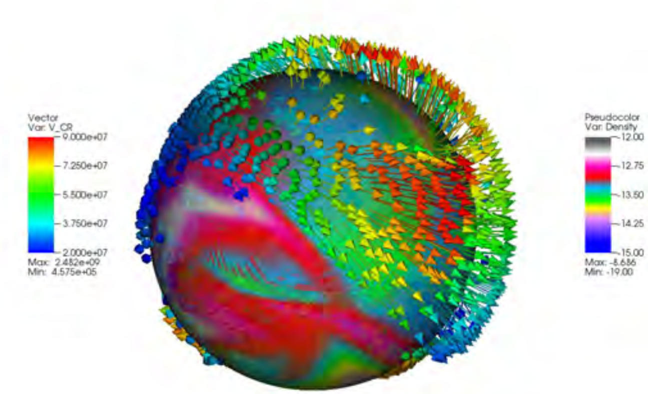

R=3e11 < r_{Shock}

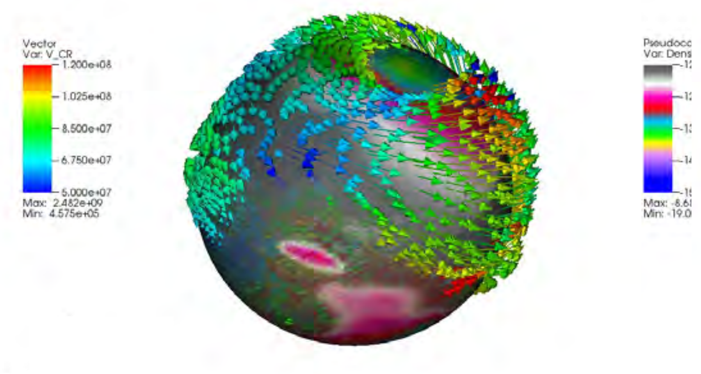

R=1.5e11

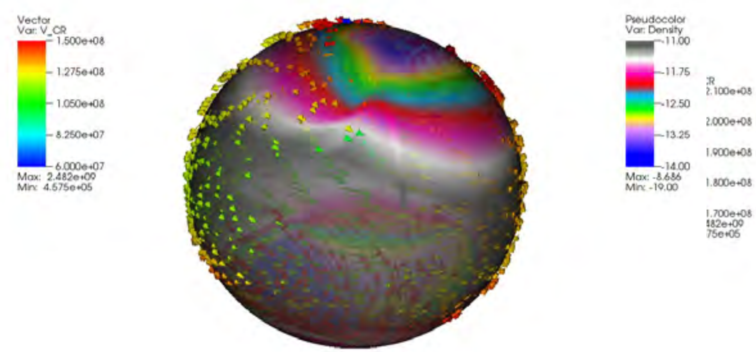

R=7.5e10

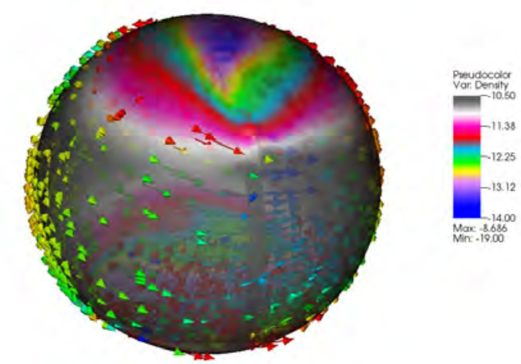

R=3e10

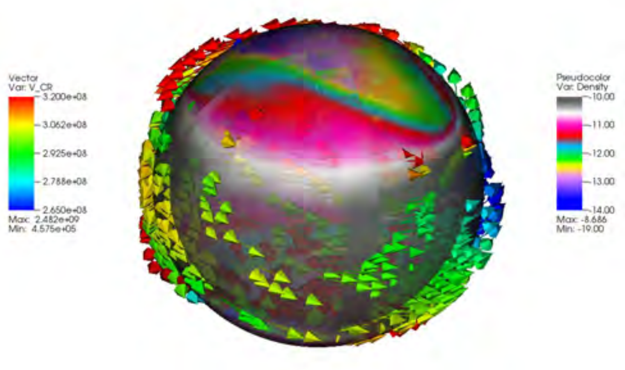

R=1.5e10

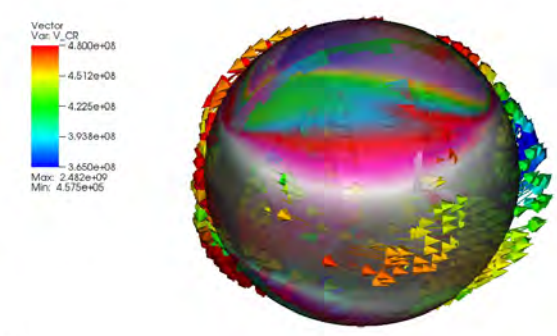

R=7.5e9

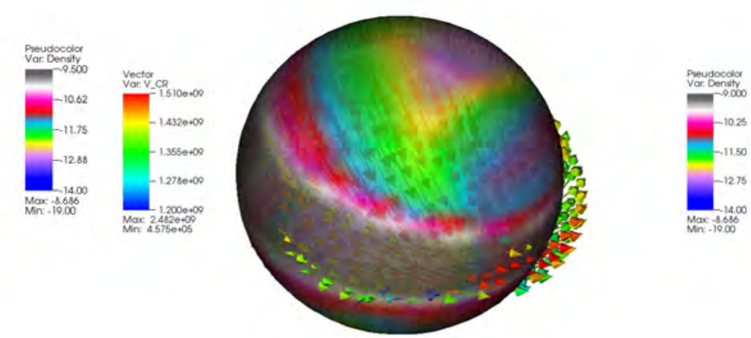

R=1.2e9

The disks form over 3 orders of magnitude to be fully present on a scale of about 250 gravitational radii.

The disk is not entirely Keplerian, has still shocks, is not uniform But may probably radiate equally than a classical disk (thermal emission)

Hydro: drain flow: low density, high velocity flow normal to the disk and towards the pole of the BH. Good conditions for jets?

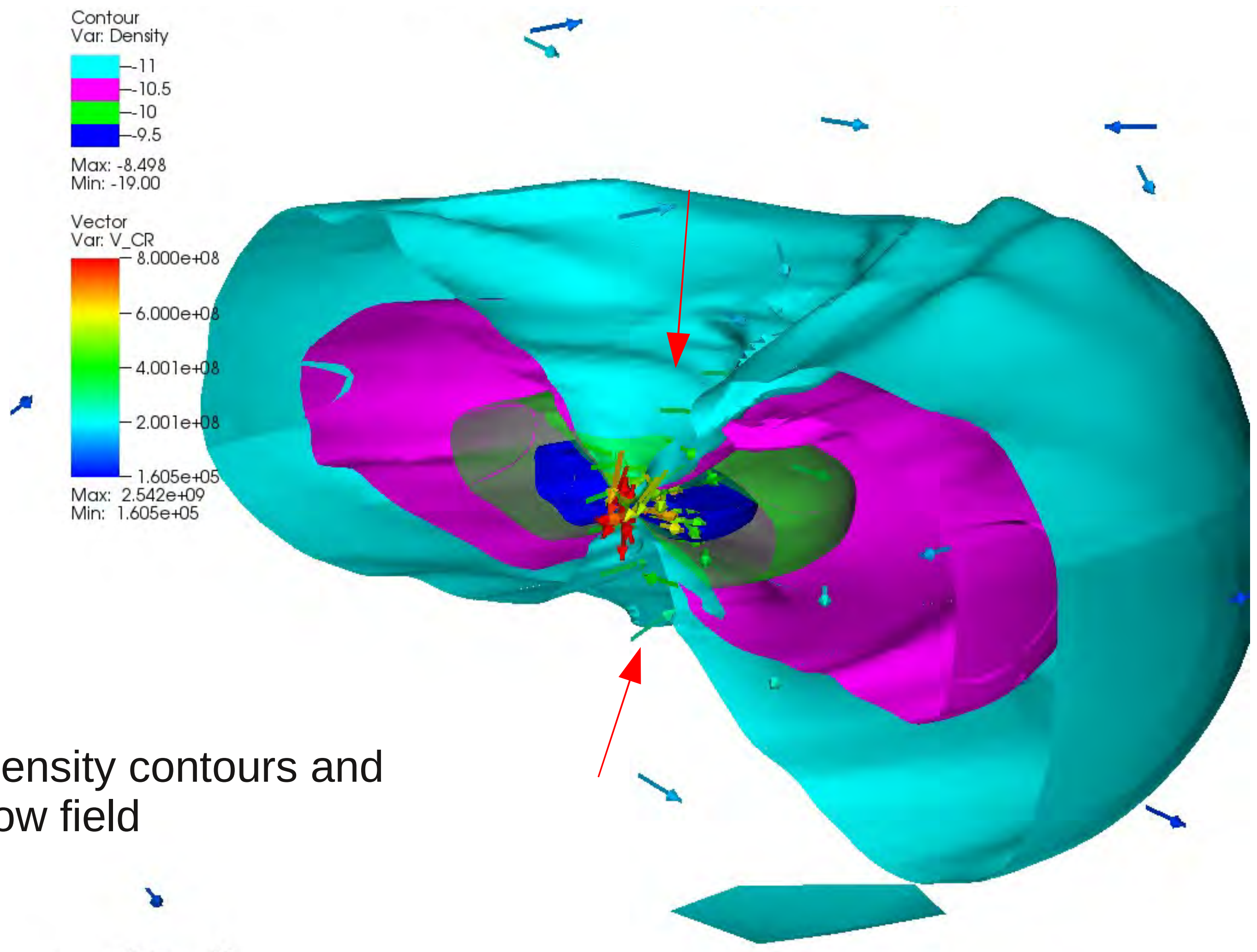

Density contours and flow field

Accretion Ball regime (v_W > 1000 km/s)

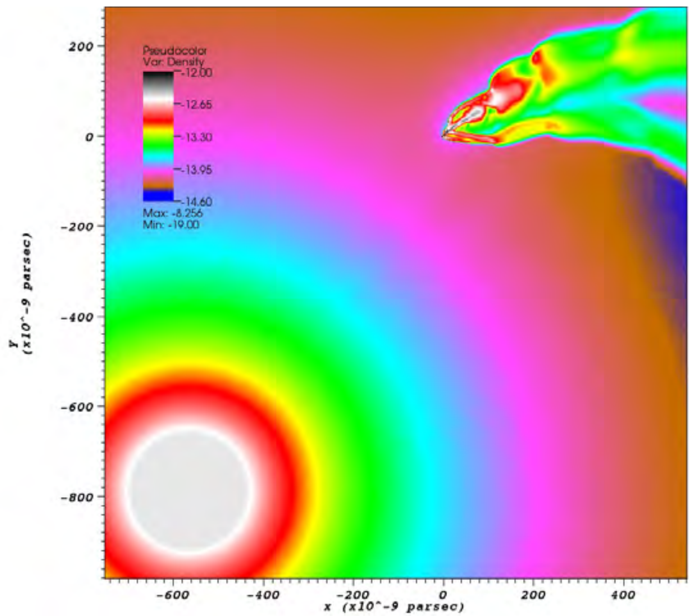

The inner dissipation region consists of a network of shocks produced by different colliding, higly supersonic streams.

High density filaments develop.

Angular momentum is essentially advected by the network of shocks.

Spinning structures may eventually develop but are transient.

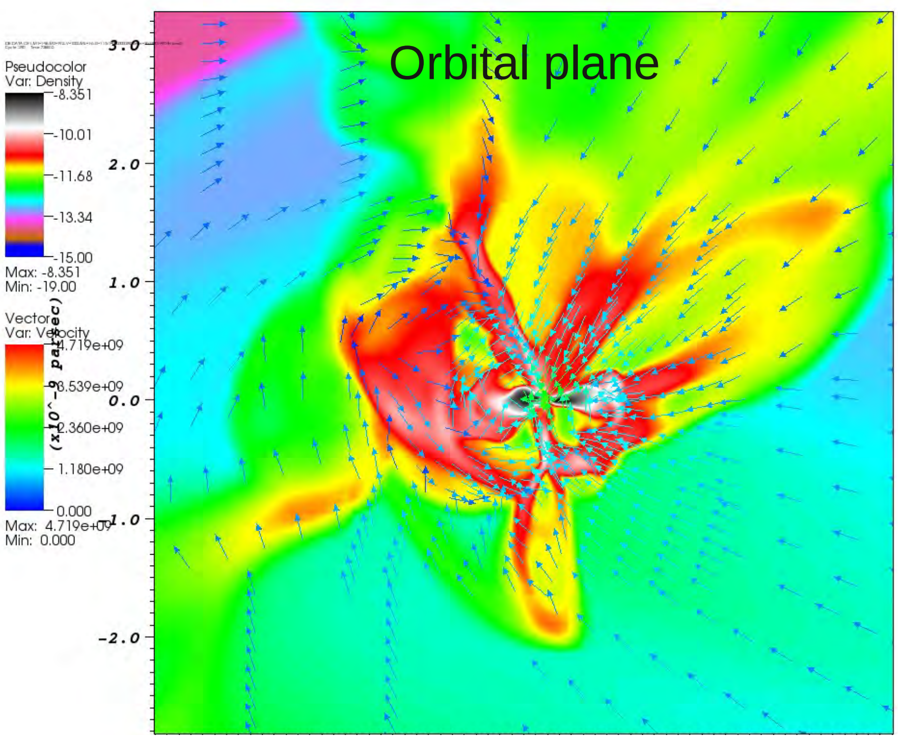

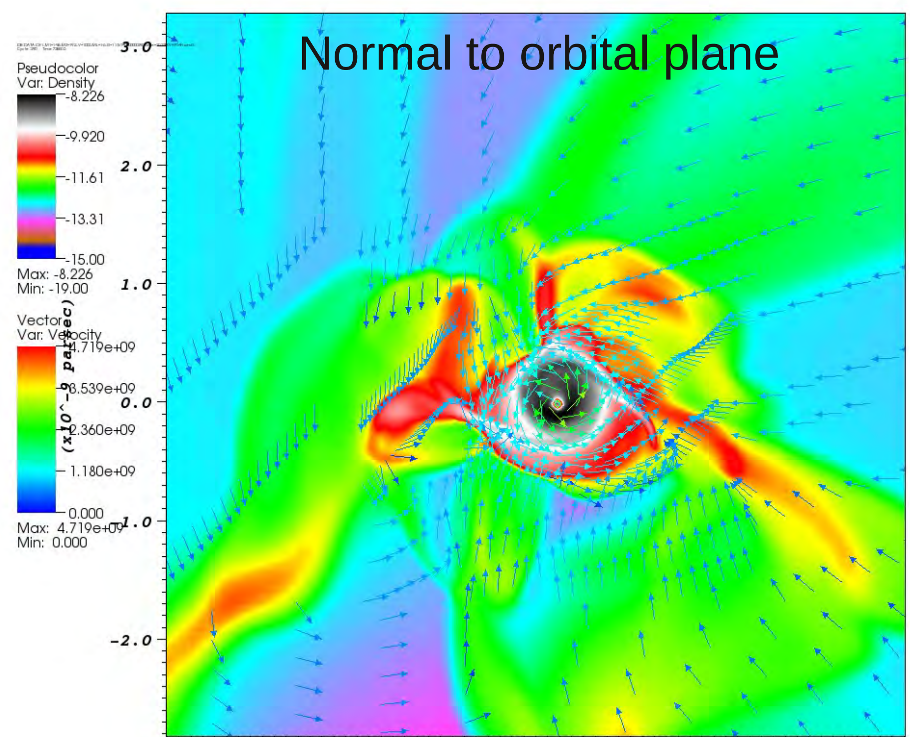

Movie of accretion ball regime

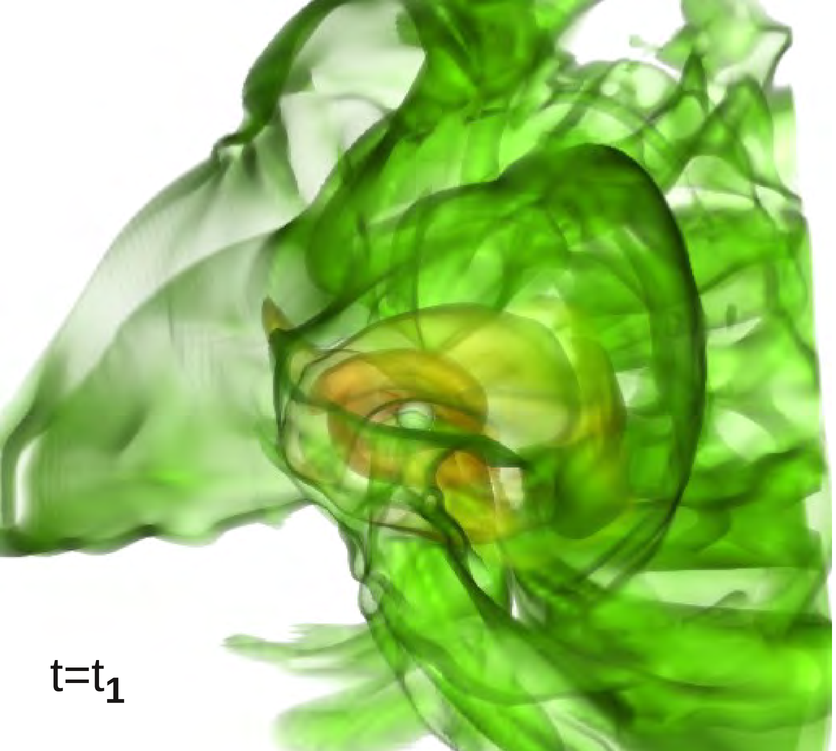

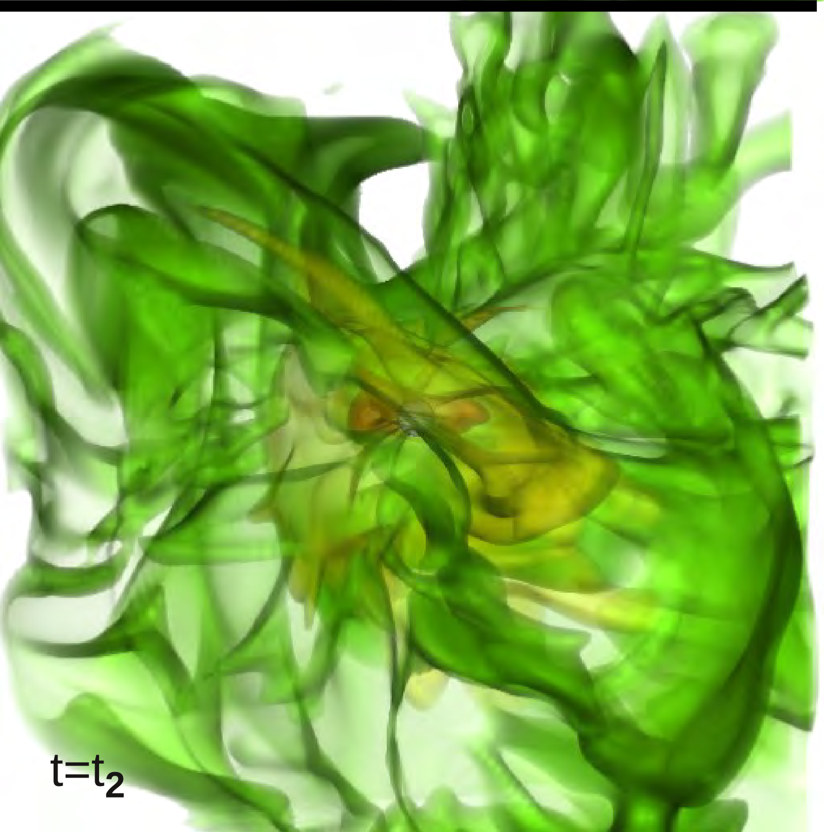

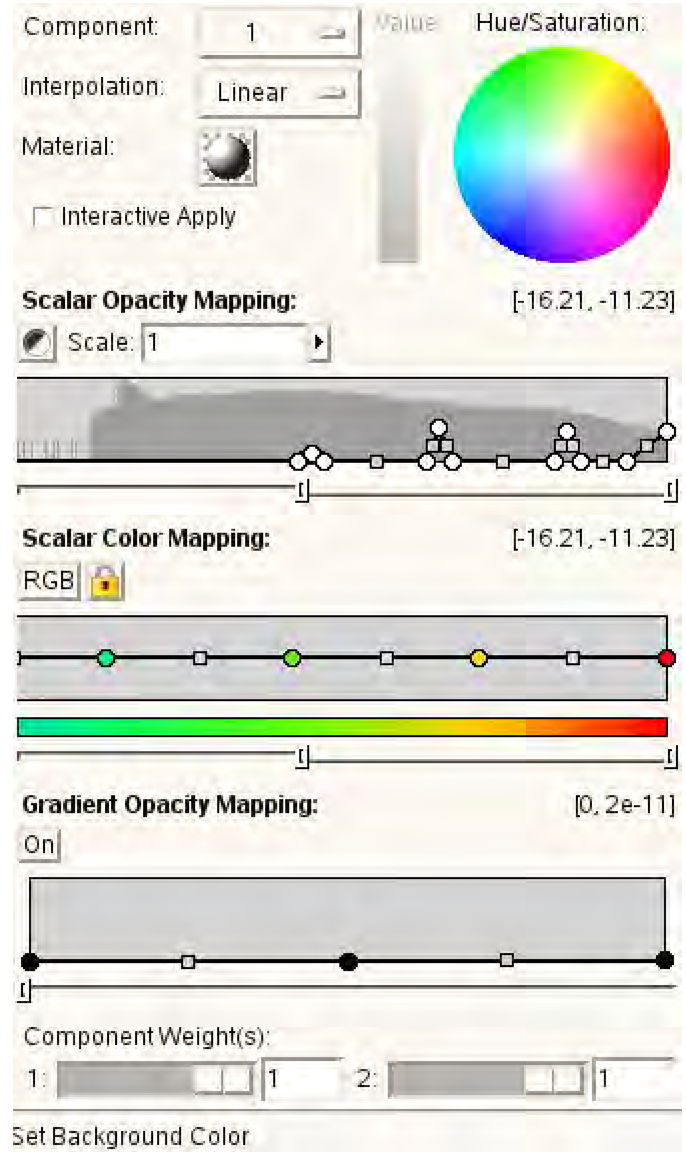

Opacity from different density values
red : $\log(\rho) = -11$
green: $\log(\rho) = -14$
blue : $\log(\rho) = -16$

Opacity from gradients

Why is no disk formed in these cases?

The dissipation process starts about 1 order of magnitude more deep in the potential well → not enough room and time to form a disk.

In particular, note that much more kinetic energy/angular momentum has to be dissipated if wake shock is deep in the well

Already the 850 km/s model shows occasionally a disk break down though it is still predominately in the disk regime.

However, it has 2 times changed the rotation direction of the disk
Pro-grade disk → accretion ball → (temporarily) retro-grade disk →
accretion ball → pro-grade disk

Is accretion ball regime dominated by non-thermal emission?

Conclusions: wind-accretion in high mass microquasars

Shocks are present everywhere

1) A spirally shaped structure is imposed on density, velocity on a circum-binary scale.

2) A shock-bound accretion wake is present on the Bondi-Hoyle scale.

3) The wake is supersonically turbulent – its orientation depends on v_W/v_O .

4) Mass accretion rates correspond approximately to the BHL rates.
However, the angular momentum accretion rates do not.

5) We have identified 2 (3?) different accretion regimes: disk (v_W< 900 km/s) and ball.
The two different states of HMXRBs (low/high) may be caused by this.
But what is the trigger for the switching?

6) All shocks are collision-less, even in the high-density disk.

7) Hydrodynamical models can account well for the low speed wind regime and
the emission from the inner disk may well explain the thermal component.

8) High speed wind models are not well described in the hydrodynamical limit as
thermalization scales approach typical dynamical scales.
Role of kinetic instabilities and turbulence?

How do we include more physics?

The example of magnetic reconnection

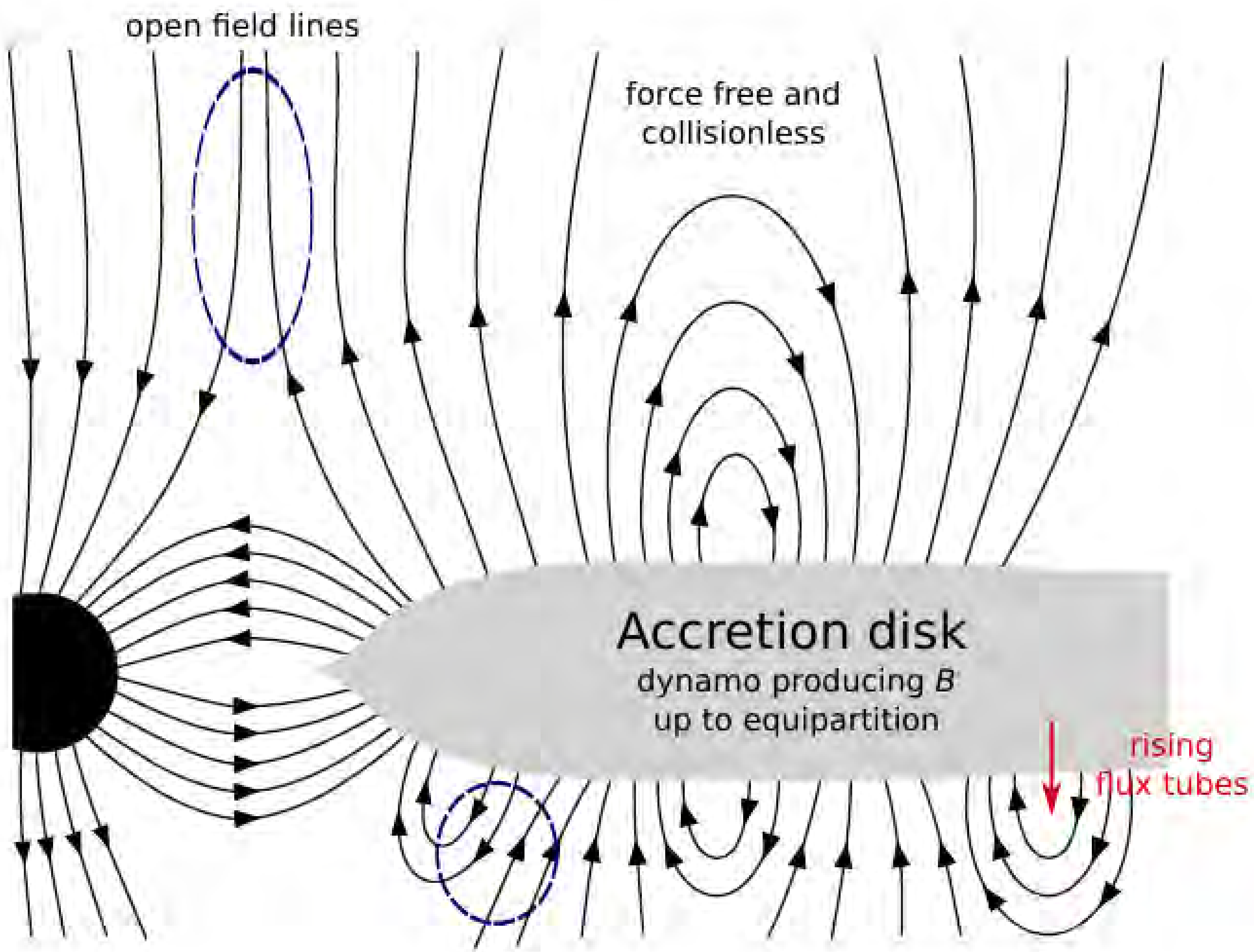

From deGouveia etal. (2005)

How do we include more physics?

The example of magnetic reconnection

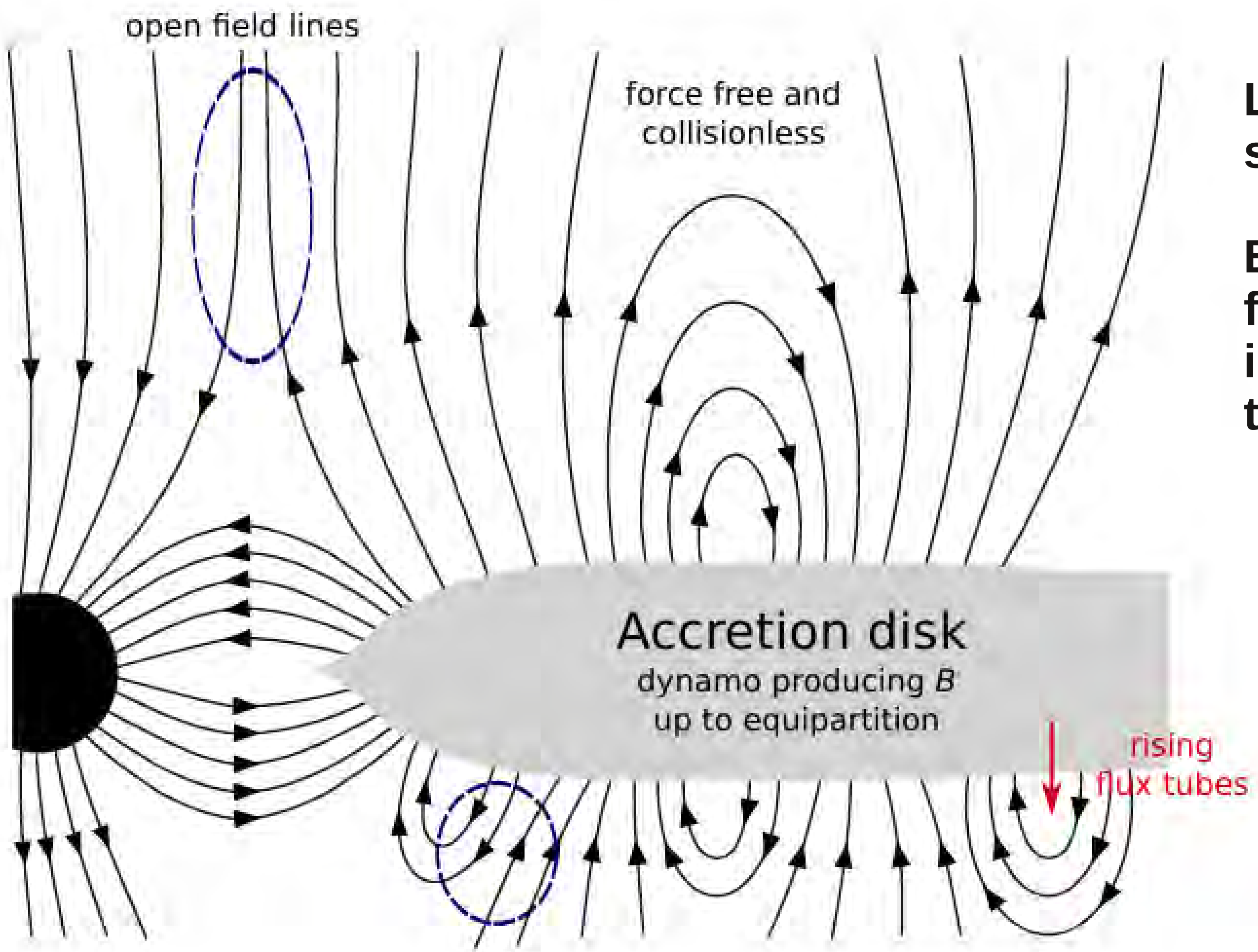

From deGouveia etal. (2005)

Large scale field and large scale reconnection events.

Besides, there is the turbulent field component (and inevitably linked to it) turbulent reconnection.

PIC simulations of relativistic magnetic reconnection

(From Melzani et al. (2013, submitted) & Melzani et al. (2013, in preparation))

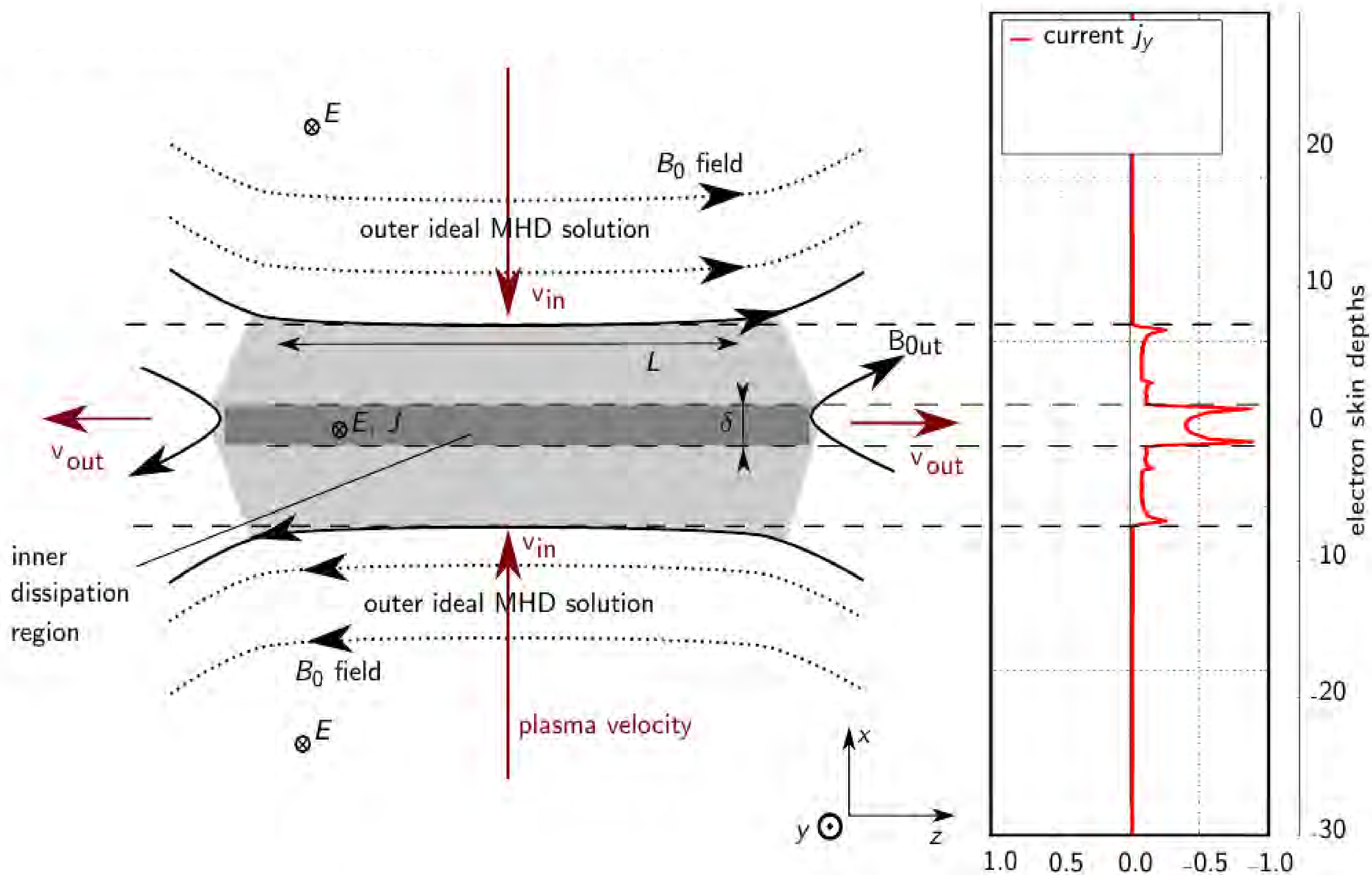

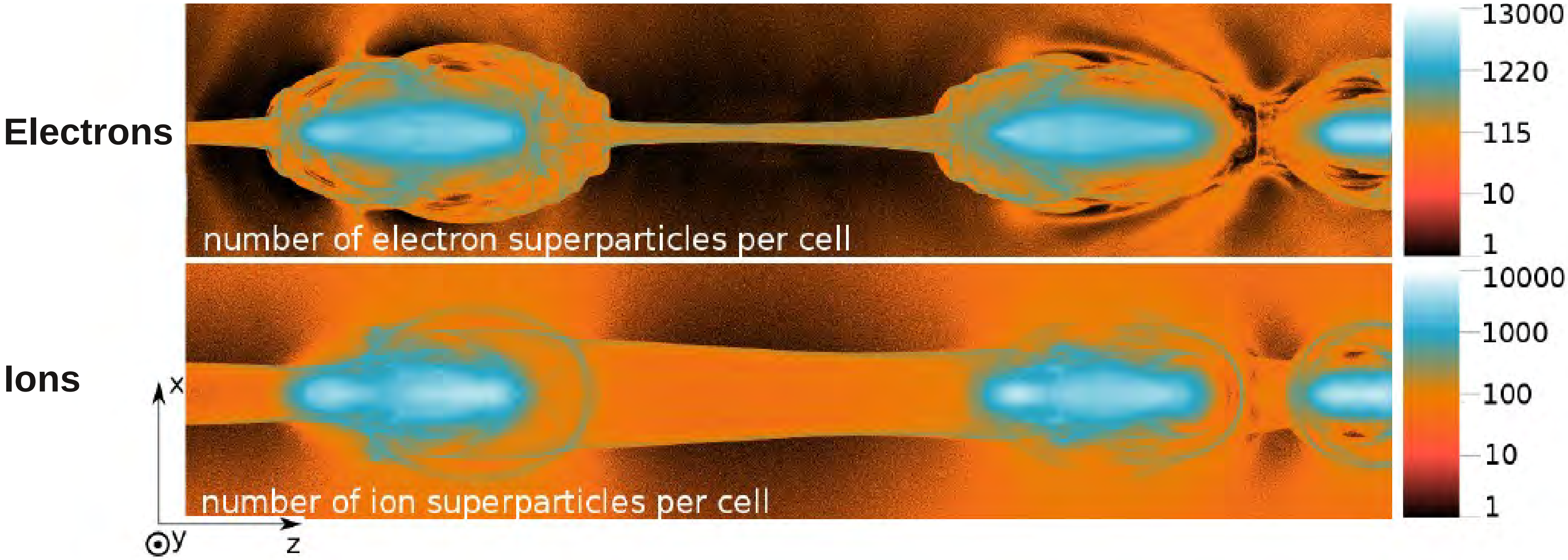

Non-ideal effects

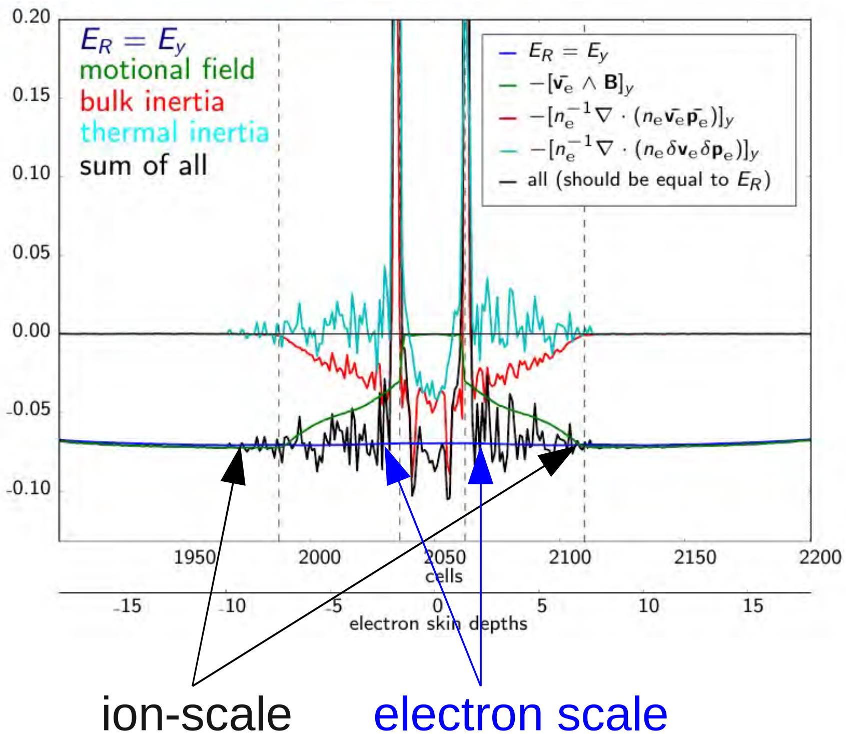

Goals of this study:

- **Fundamentals of magnetic reconnection**
- **Scales on which we have non-ideal effects**
- **Derive transport coefficients to be included into non-ideal MHD**

PIC simulations of relativistic magnetic reconnection

(From Melzani et al. (2013, submitted) & Melzani et al. (2013, in preparation)

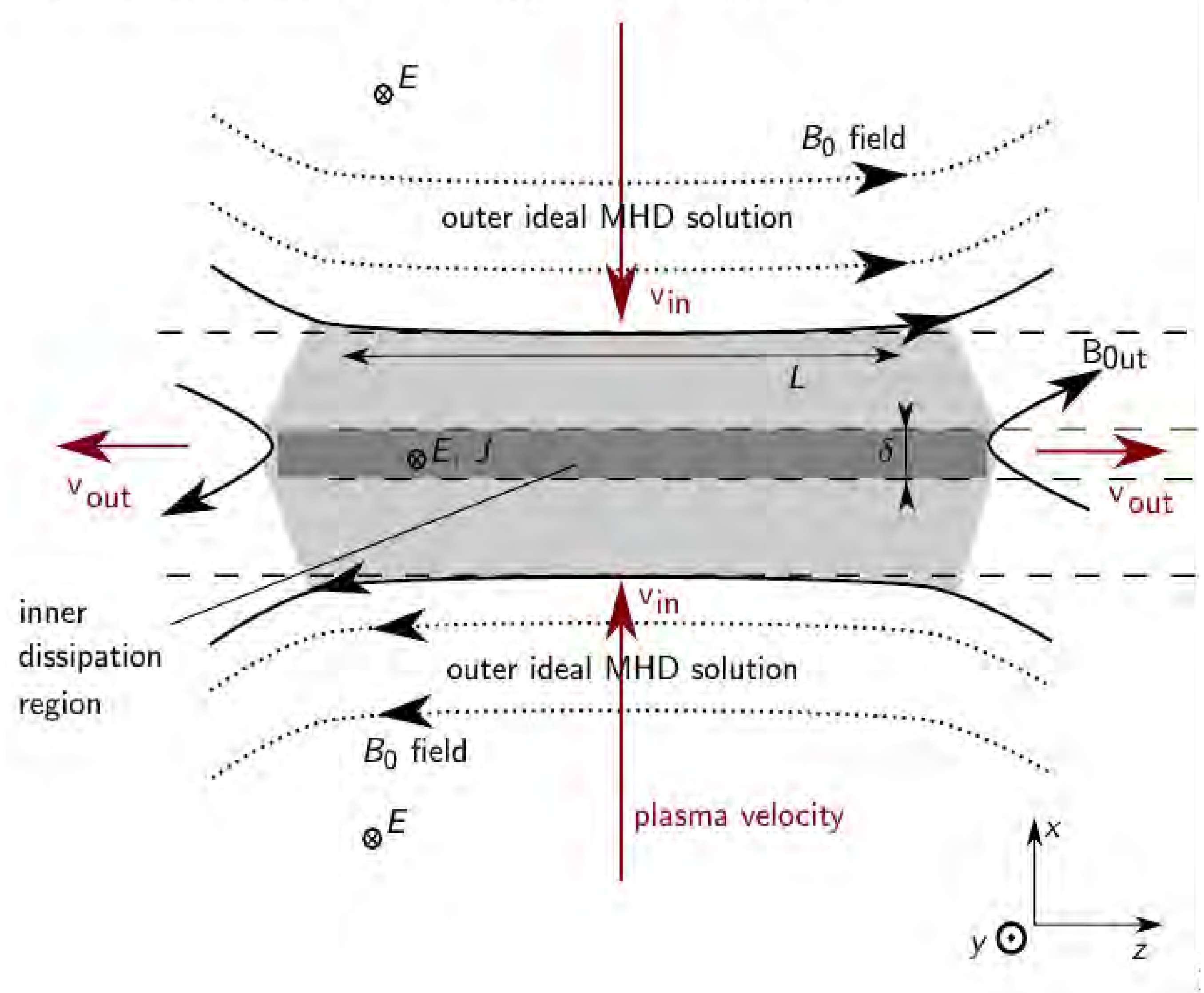

Outer region

Compute outer solution on the basis of ideal MHD,

or better,

on the basis of non-ideal MHD with an appropriate sub-grid-scale model

Inner region

Compute inner solution on the basis of a kinetic model

The project A-MAZE

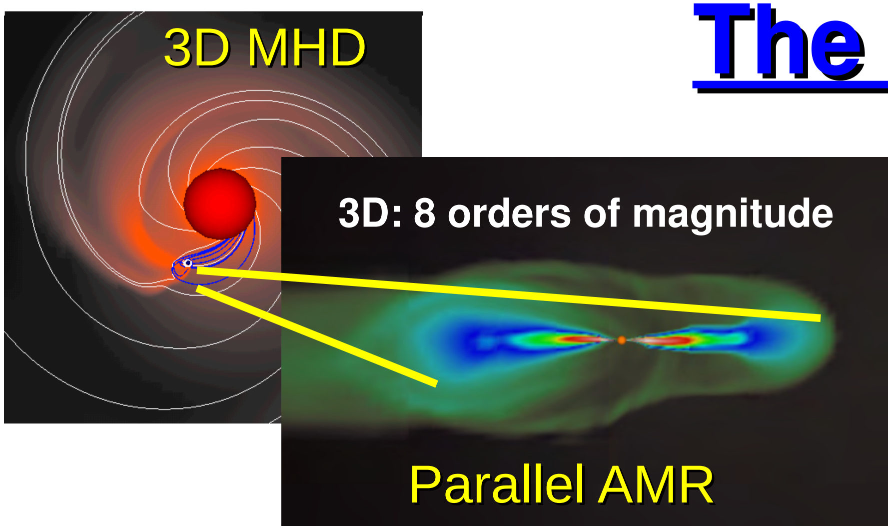

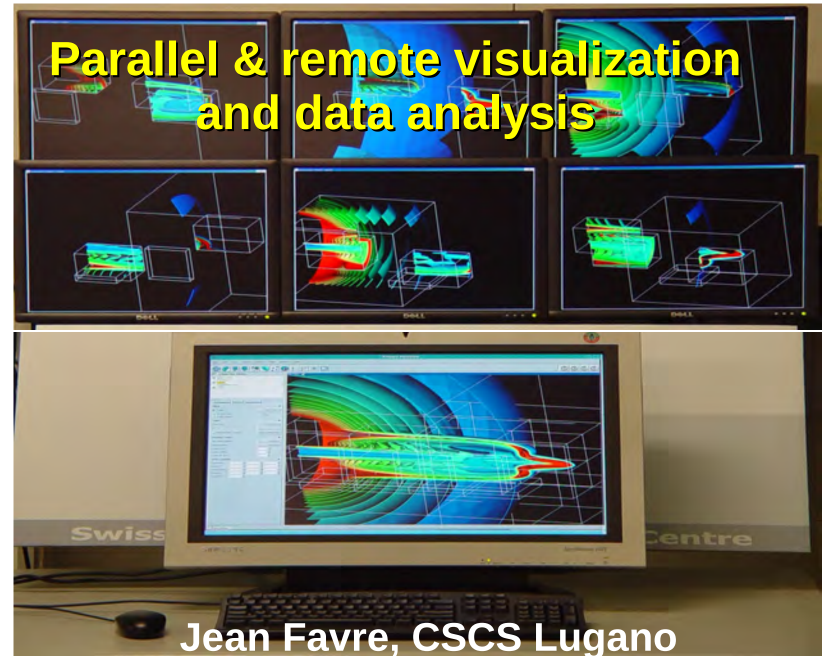

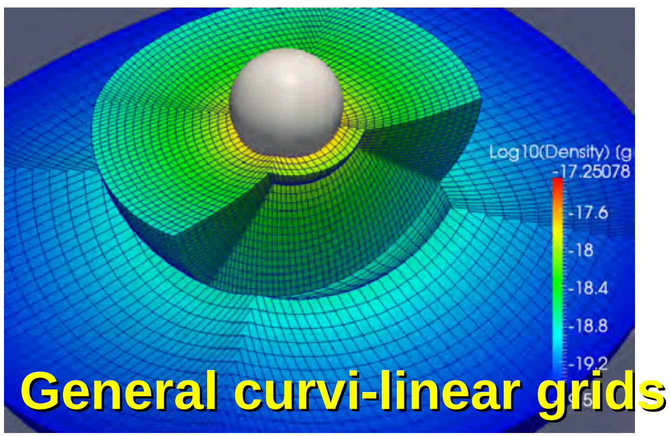

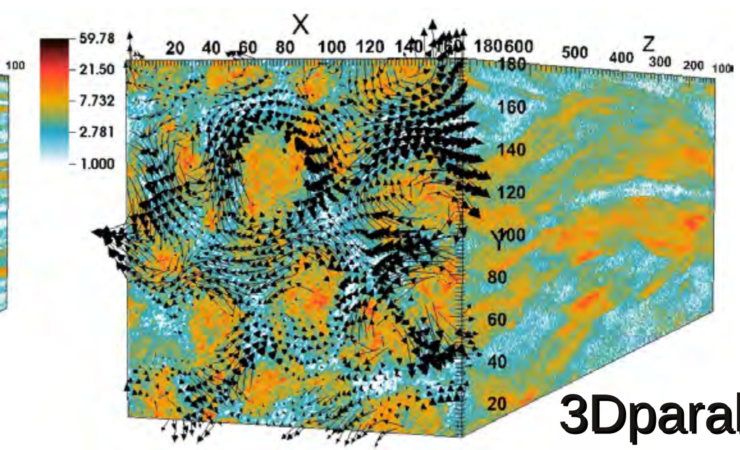

3D parallel adaptive radiative transfer code
(Boltzmann equation)

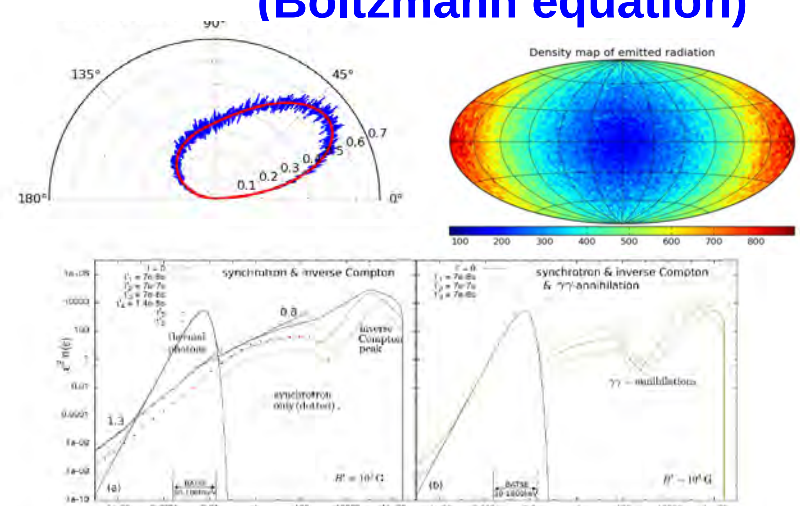

The project A-MAZE

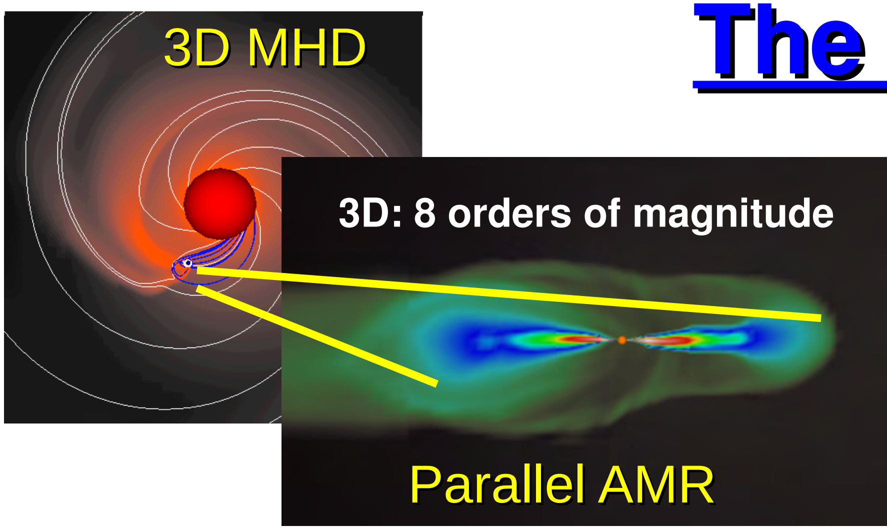

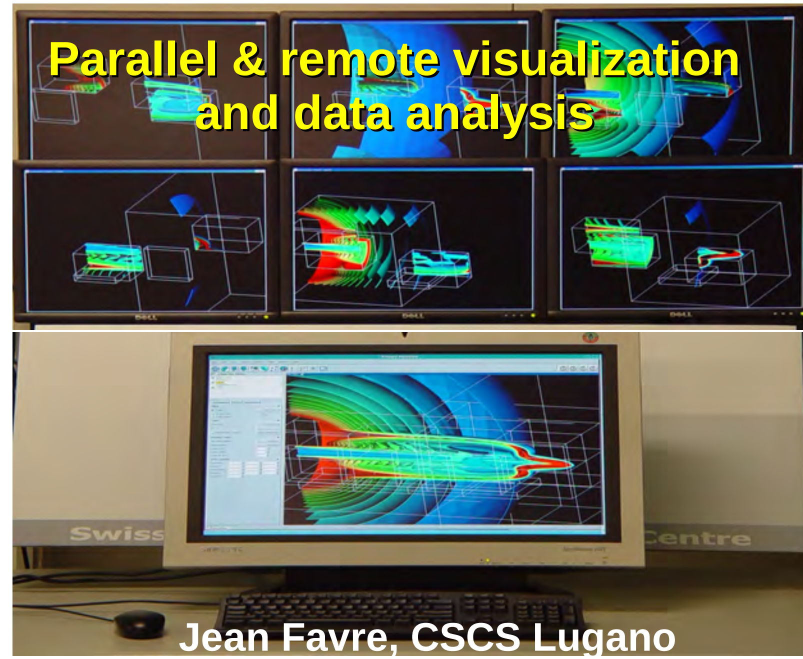

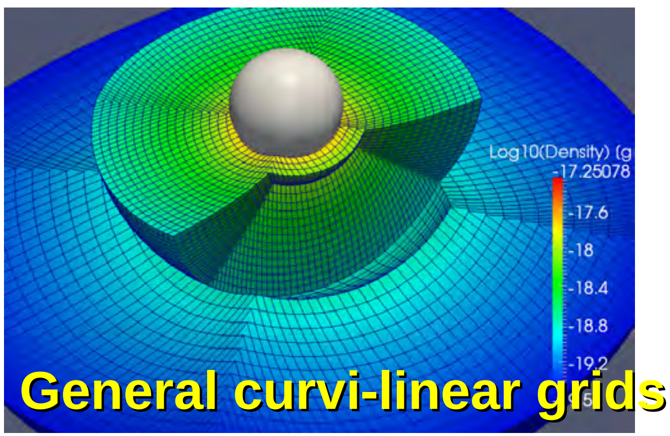

3D parallel adaptive radiative transfer code
(Boltzmann equation)

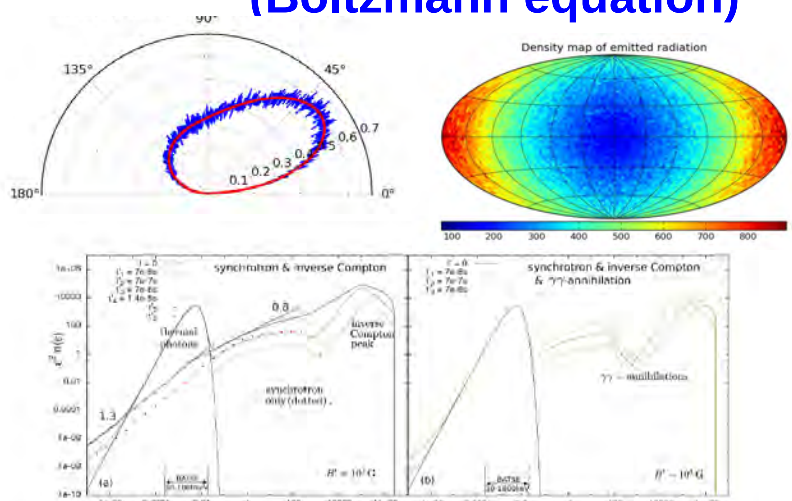

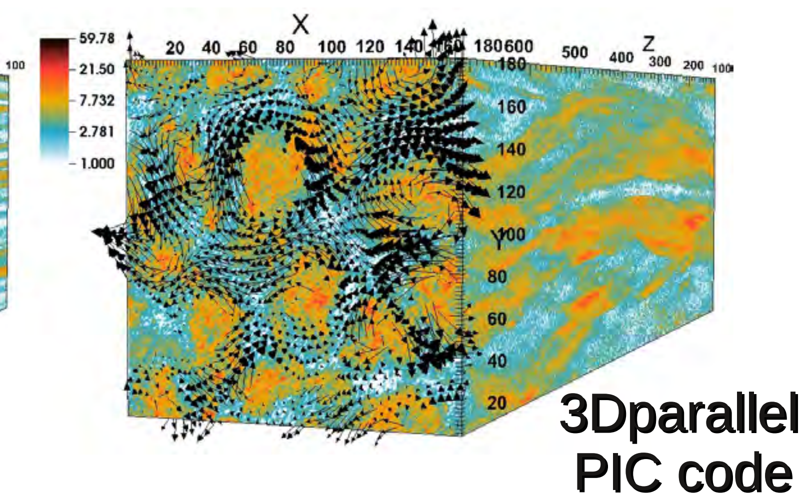

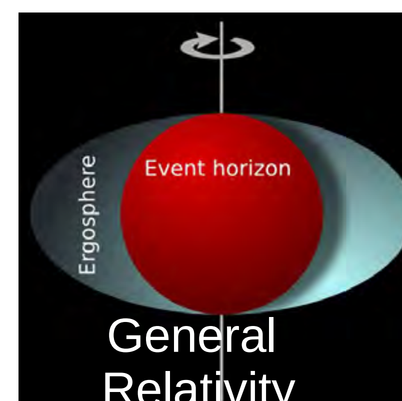

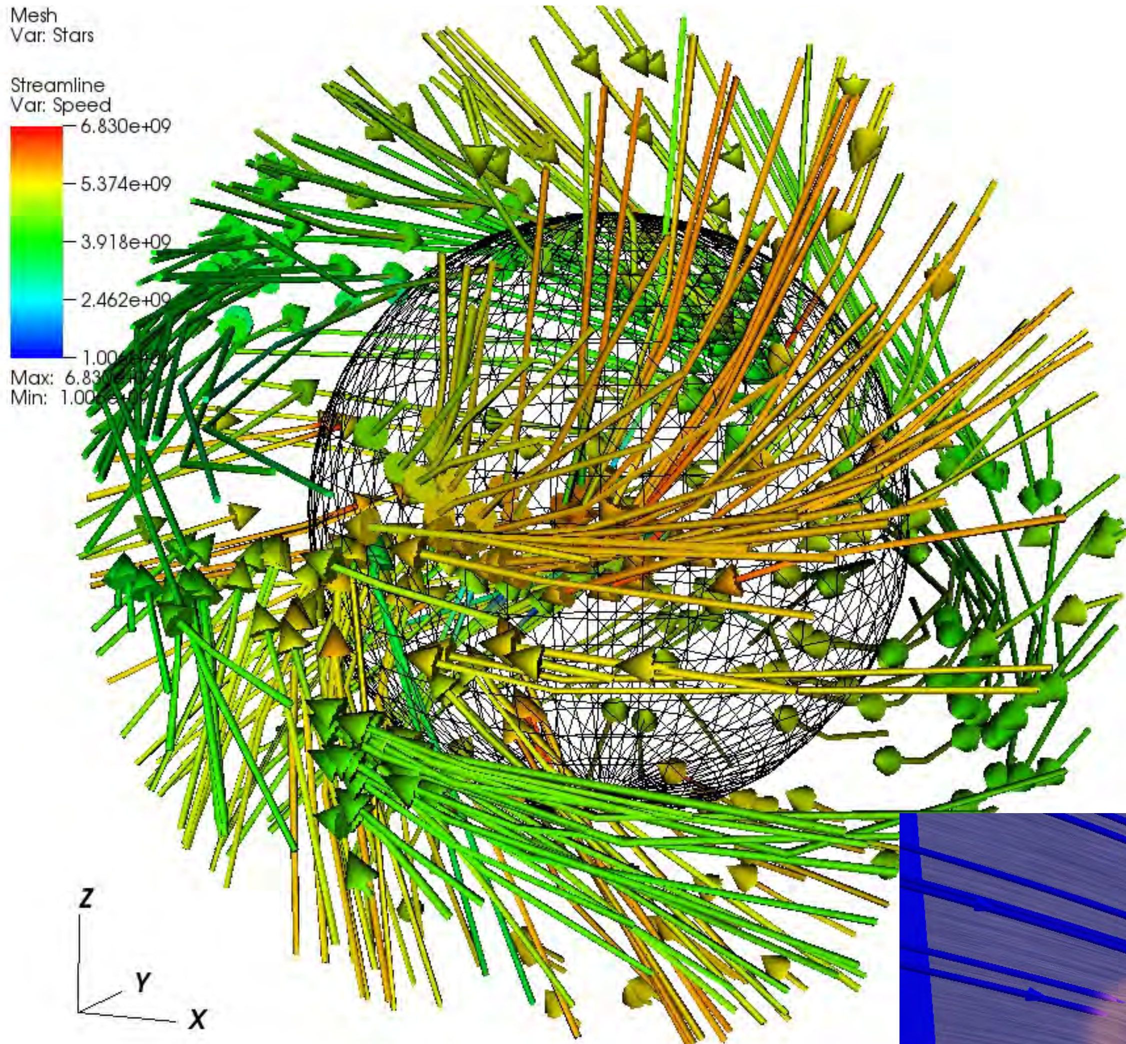

The swirling end